MJO modulation of TC genesis: An intraseasonal genesis potential index

Bin Wang and Ja-Yeon Moon

Department of Atmospheric Sciences and IPRC,
University of Hawaii at Mañoa, Honolulu, HI, USA

1-23 2017 AMS Seattle

MJO Impacts – Tropical Cyclones

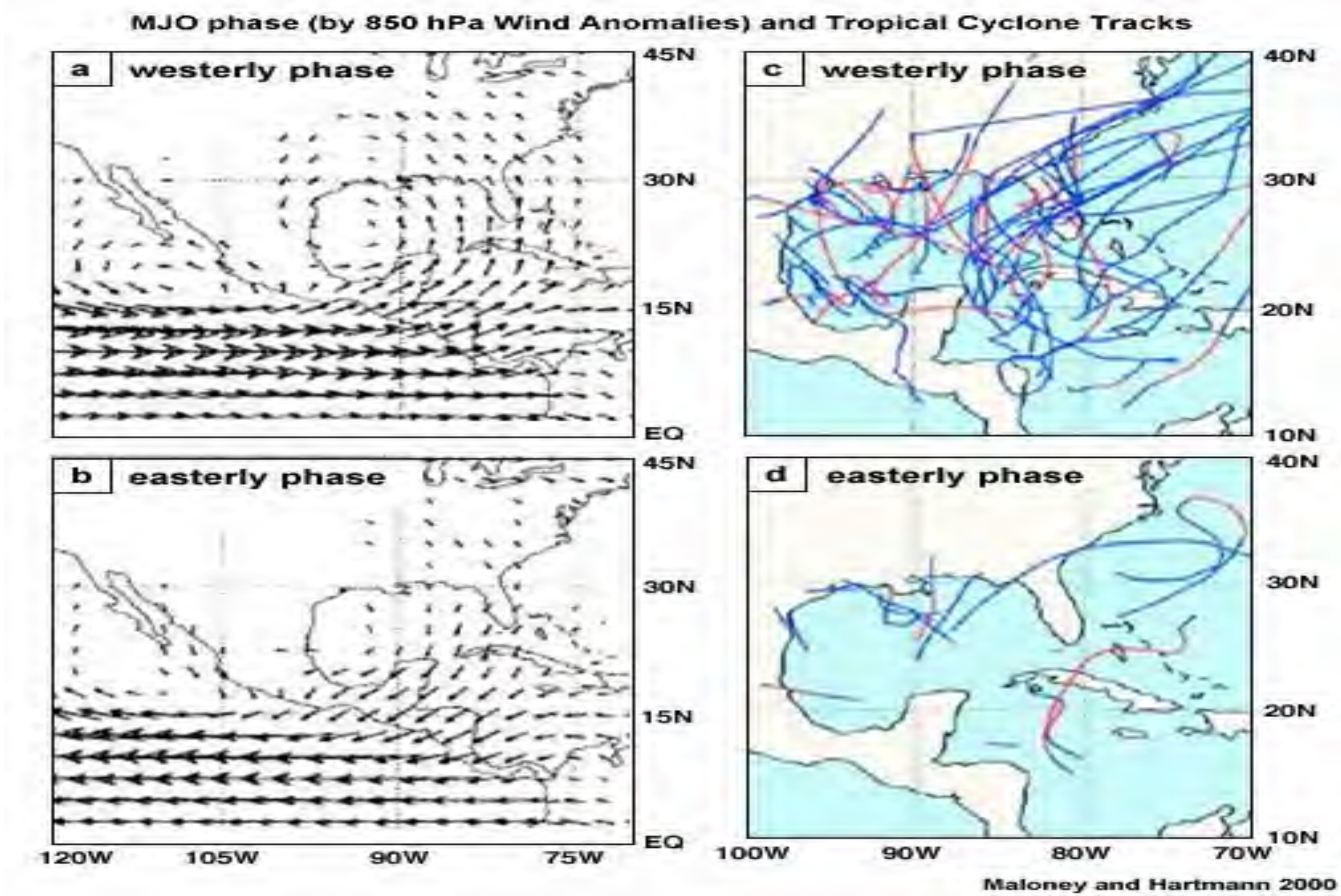

The MJO often leads to “bursts” and “lulls” in tropical cyclone activity when active periods general ly last for about two weeks due to changes in both lower and upper-level winds and convection

Maloney and Hartmann 2000

MJO Impacts on TC rapid intensification in WNP

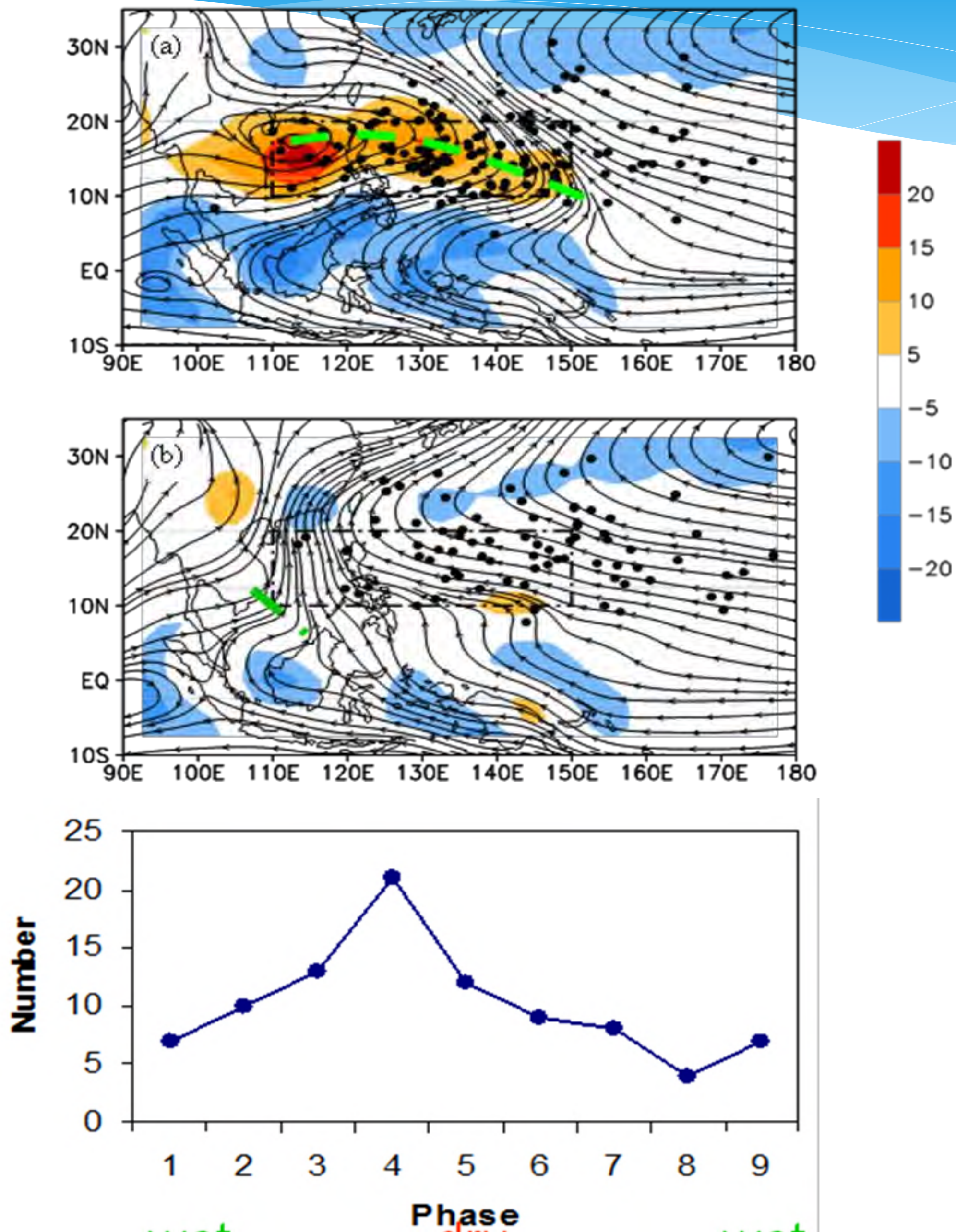

Wang and Zhou 2008

Empirical studies have qualitatively established the effects of MJO on TCG

A. North Indian Ocean
Liebmann et al. 1994, Kikuchi and Wang 2010, Krishnamohan et al. 2012

B. Western North Pacific Nakazawa 1988, Liebmann et al. 1994, Wang and Zhou 2008, Kim et al. 2008, Li and Zhou 2013

E. Southern Indian Ocean
Bessafi and Wheeler 2006, Ramsay et al. 2012

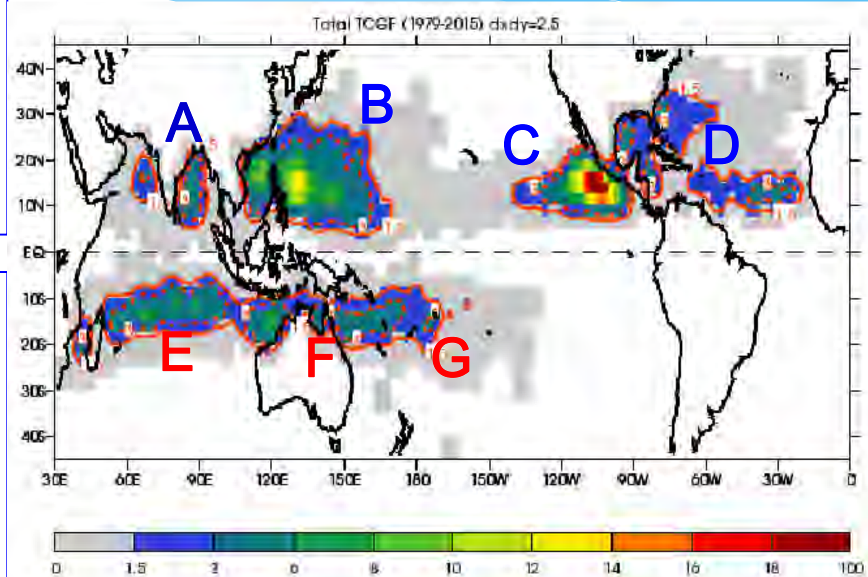

C. Eastern North Pacific
Molinari et al. 1997, Maloney and Hartmann 2000a, Aiyyer and Molinari 2008

D. Gulf of Mexico and North Atlantic
Maloney and Hartmann 2000b, Barret and Leslie 2009

G. South Pacific Ocean Chand and Walsh 2010

F. Australian region
Hall et al. 2001

MJO has been recognized as a strong modulator to TC activity in global ocean basins since late 1980s.

The quantitative diagnostic studies based on Emanuel-Nolan GPI

Emanuel-Nolan (2004) genesis potential index (GPI):

$$\mathrm{ENGPI} = |10^5\eta|^{3/2}\left(\frac{RH}{50}\right)^3\left(\frac{V_{pot}}{70}\right)^3(1+0.1V_{shear})^{-2}$$

Camargo et al. (2009) found

1. ENGPI captures the annual cycle of TC genesis very well but less well in describing MJO modulation of TCG.
2. Among the four factors, the RH makes the largest contribution.

Issues:

a. The RH is often a result of circulation anomaly. What is the rudimentary process by which MJO modulates TCG.

b. The ENGPI were derived from climatology. It is not clear whether it can be fully applicable to depict intraseasonal variation of the TCG.

Our work

- Identify major circulation factors associated with MJO that affect the global TCG potential.
- Establish an empirical intraseasonal GPI (ISGPI) linking MJO and TCG anomalies.
- Elaborate the major processes by which MJO controls TCG potential.
- Explore applicability and performance of the ISGPI in reproducing observed IS TCG variability.

Intraseasonal OLR variance and TC genesis

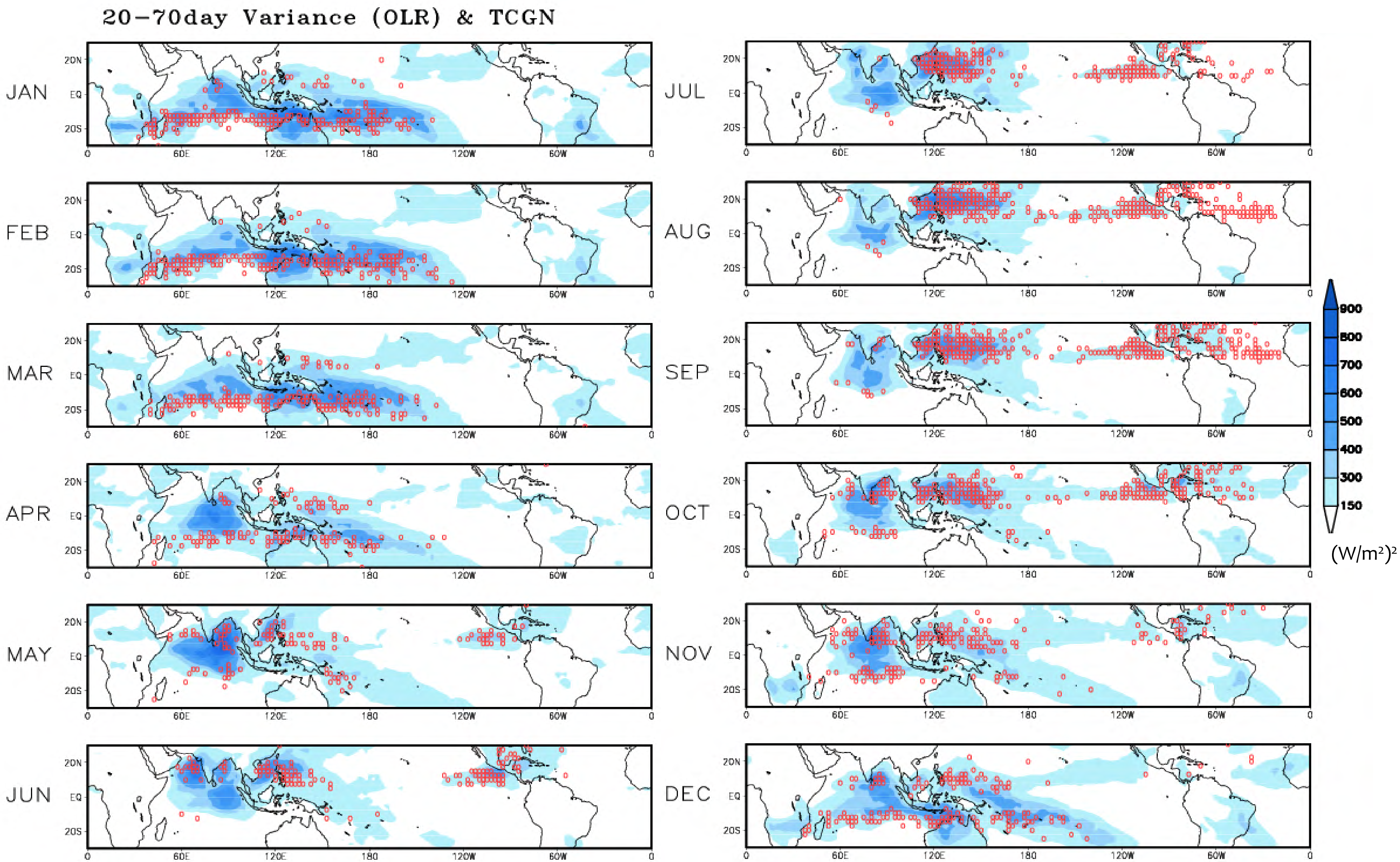

Data

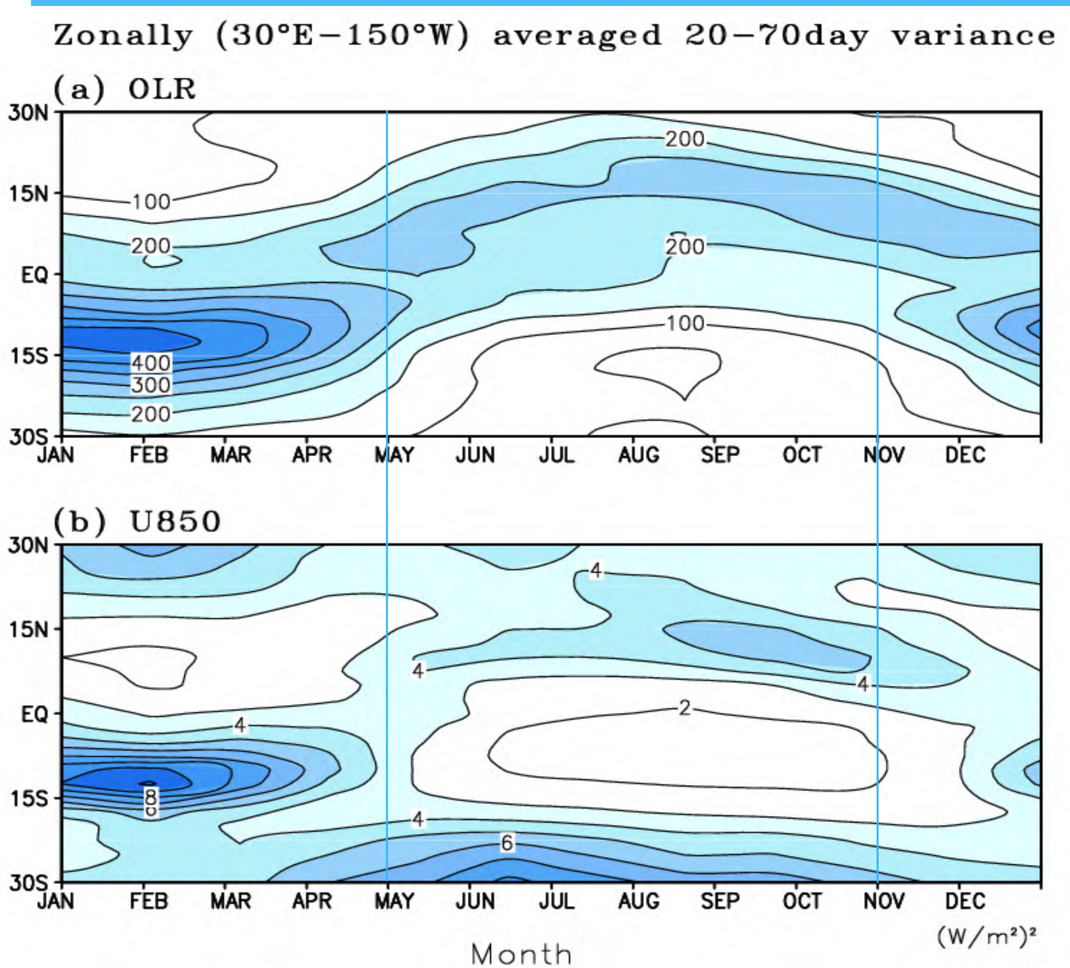

Fig. Climatological mean zonally averaged 20-70 day variance of (a) OLR and (b) zonal wind at 850hPa (U850) between 30°E and 150°W as functions of calendar month and latitude from 30°S to 30°N.

- ✓ Basis for the seasonal stratification

The evolutions of OLR and U850 suggests that transition seasons are: April-May and November-December!

In this study, Austral summer tropical cyclone season is defined as November through the next April (NDJFMA).

Data

* **Period of study: 1979-2014** ,
* Boreal winter from November-April
* **TC dataset:** IBTrACS; http://www.ncdc.noaa.gov/ibtracs) v03r06 from (Knapp et al. 2010).
* TC genesis: maximum sustained wind speed of 34 knots (17 ms^{-1}).
* 20~70 day Lanczos band-pass filtered daily OLR from NOAA and circulation variables from ERA-Interim.

Deriving the intraseasonal TC GPI

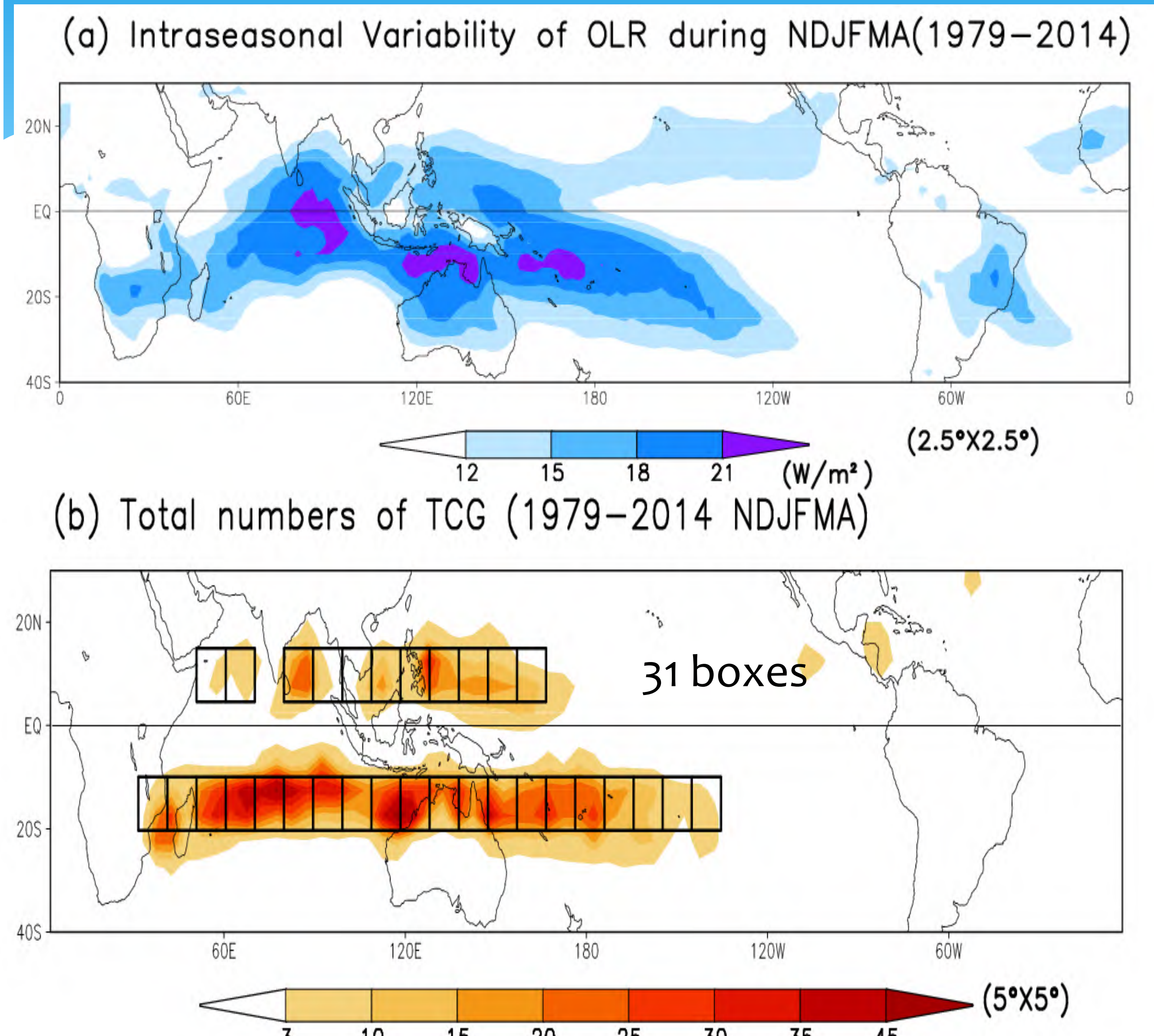

- Focus on 0-20S: define an austral summer MJO index: using first two leading EOF modes OLR anomaly over 0°-360°, 0°-20°S.

- TCG occurs mainly: 10°S-20°S and 5°N-15°N, selected 10×10 degree boxes (31 boxes) along the two latitude bands.
- The sample size is 31×8=248.

MJO evolution during Austral summer

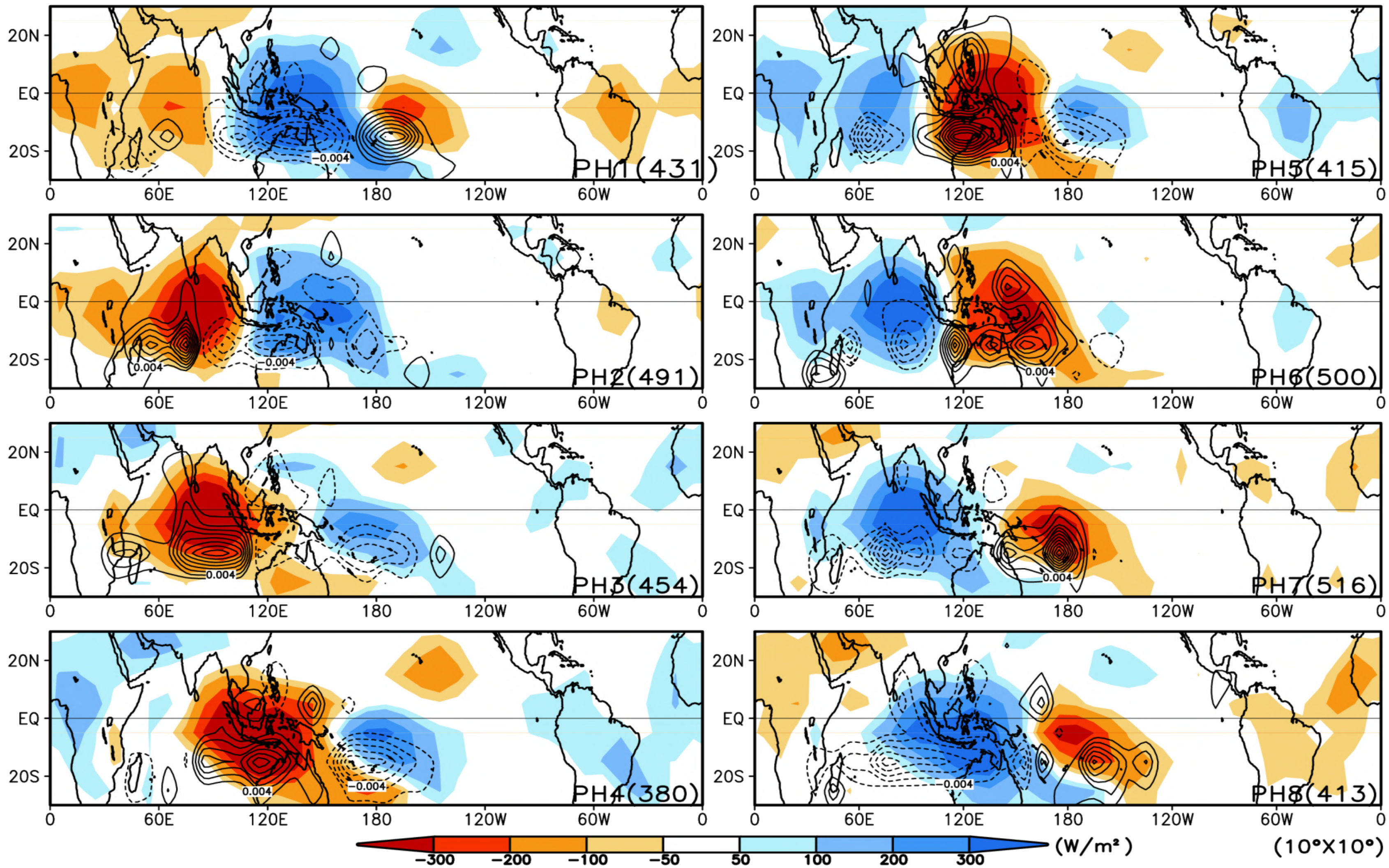

MJO Convection Center is located at Indian Ocean on phase 2-3; the MC on phase 4-5; the Western Pacific on phase 6-7.

Thinking beyond the EN GPI factors: Candidate large-scale environmental factors

Abbreviation	Description
V_{pot} (m s^{-1}),	Maximum potential intensity
SST_a (K)	Sea surface temperature anomaly relative to tropical (30°S-30°N) mean SST
RH_{600} (%)	Relative humidity at 600hPa
U_{x850} (s^{-1})	Zonal gradient of zonal wind at 850hPa
U_{y500} (s^{-1})	Meridional gradient of zonal wind at 500hPa
V_{zs} (m s^{-1})	Zonal component of vertical wind shear between 200 and 850hPa
V_s (m s^{-1})	Total vertical wind shear between 200 and 850hPa
η_{850} (s^{-1})	Absolute vorticity at 850hPa
$f\zeta_{r850}$ (s^{-2})	Relative vorticity at 850hPa weighted by the Coriolis parameter
ω_{500} (Pa s^{-1}),	Vertical p-velocity at 500hPa

Stepwise regression with F-test was used for deriving an anomalous GPI for IS variations of TCG (NDJFMA)

MJO	V_{pot}	SST	RH_{600}	U_{x850}	U_{y500}	V_{zs}	V_s	$f\zeta_{r850}$	w_{500}
R	-0.28	-0.14	0.55	-0.25	-0.54	-0.42	-0.01	0.73	-0.66
R(RH, W500)=-0.92									
20°S-EQ						**0.81** 3		**0.73** 1	**0.80** 2

$$ISGPI = (0.68)^* f\zeta_{r850} + (-0.37)^* \omega_{500} + (0.19)^* V_{zs}$$

- The vertical shear Vs and MPI V_{pot} are not important!
- RH600 is the best among ENGPI factors but highly related to W_{500} (r=-0.92)
- Vertical shear of zonal winds is better than the total wind shear

What does $f\zeta_{r850}$ *mean?*

Relative vorticity generation

at off-equatorial region

$f > \zeta_{r850}$

$D850 \sim \zeta_{r850}$

Thus,

$(f + \zeta_{r850}) \times D850 \sim f\,\zeta_{r850}$

Why is the Relative Vorticity better than RH?

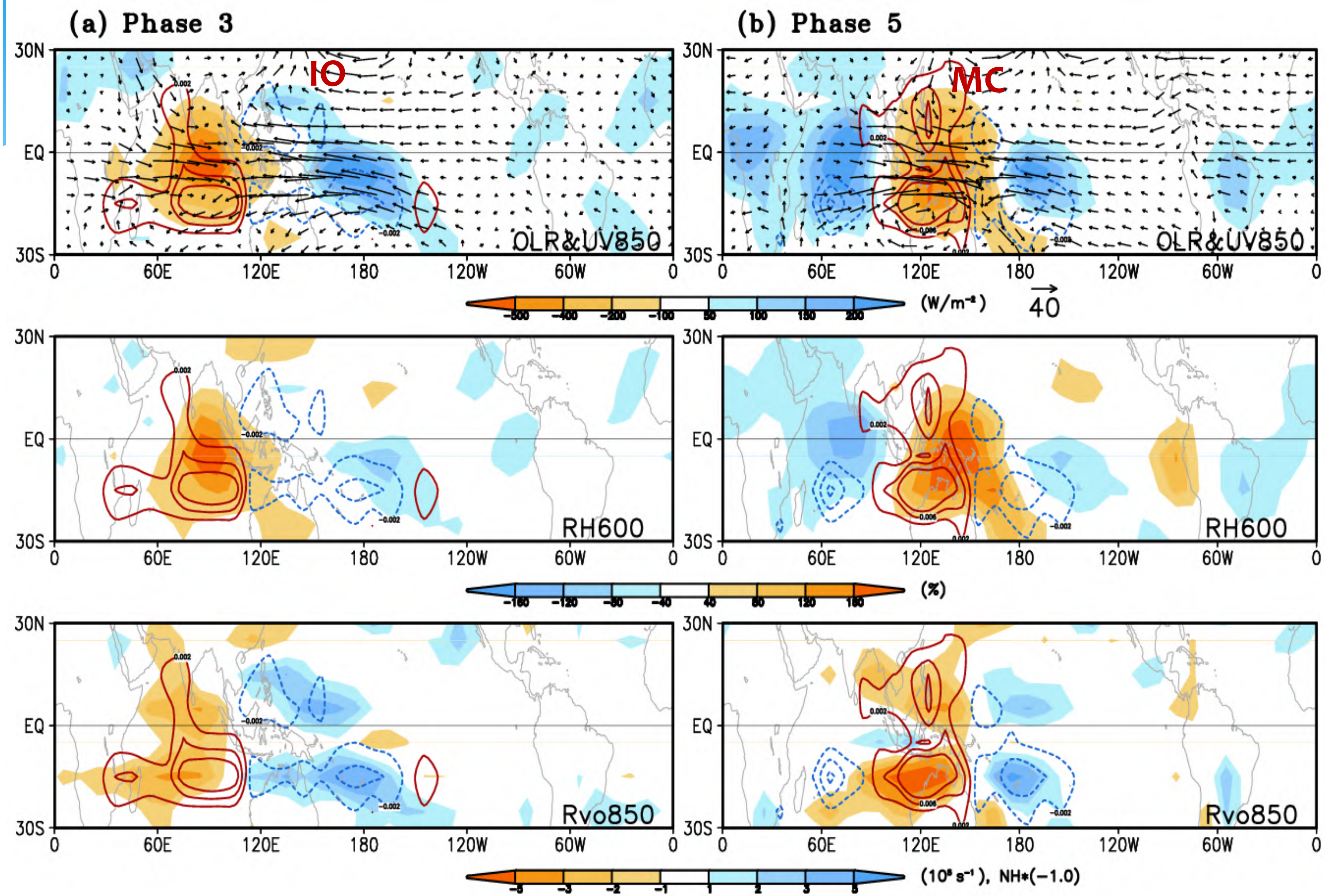

Simulation skills of the ISGPI

using three different MJO indices.

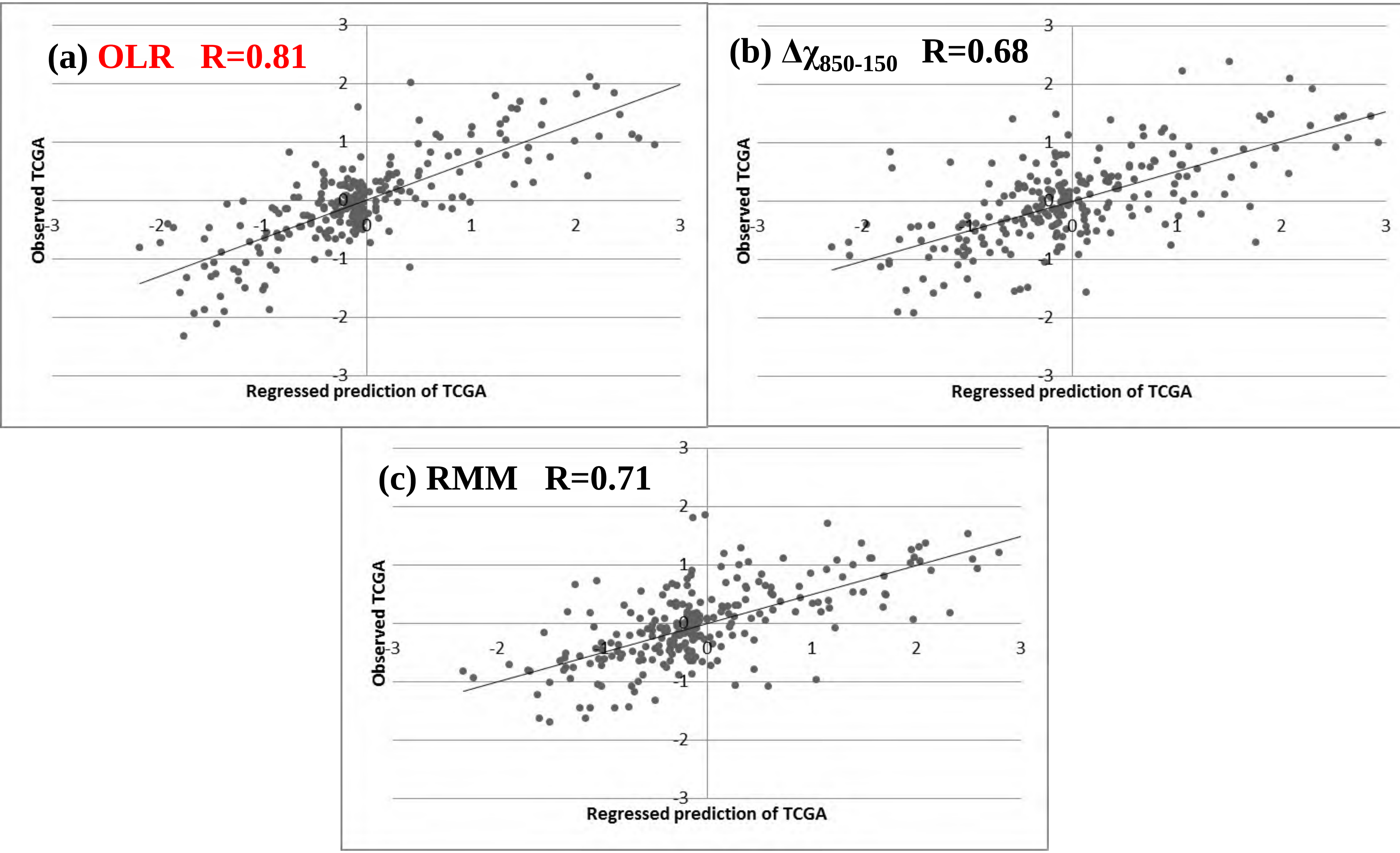

Performance along the major TCG zone (10S-20S)

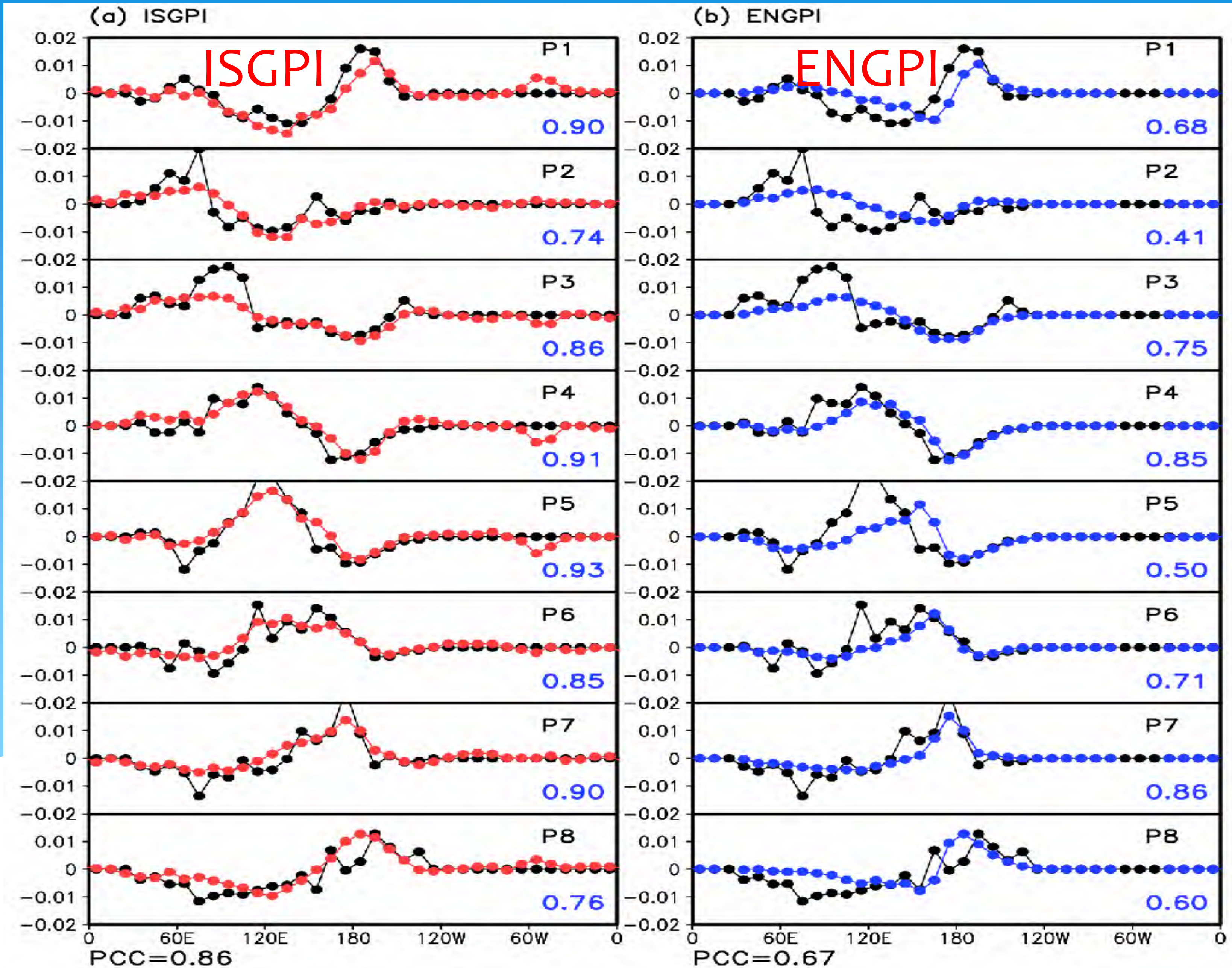

Performance in three sub-regions

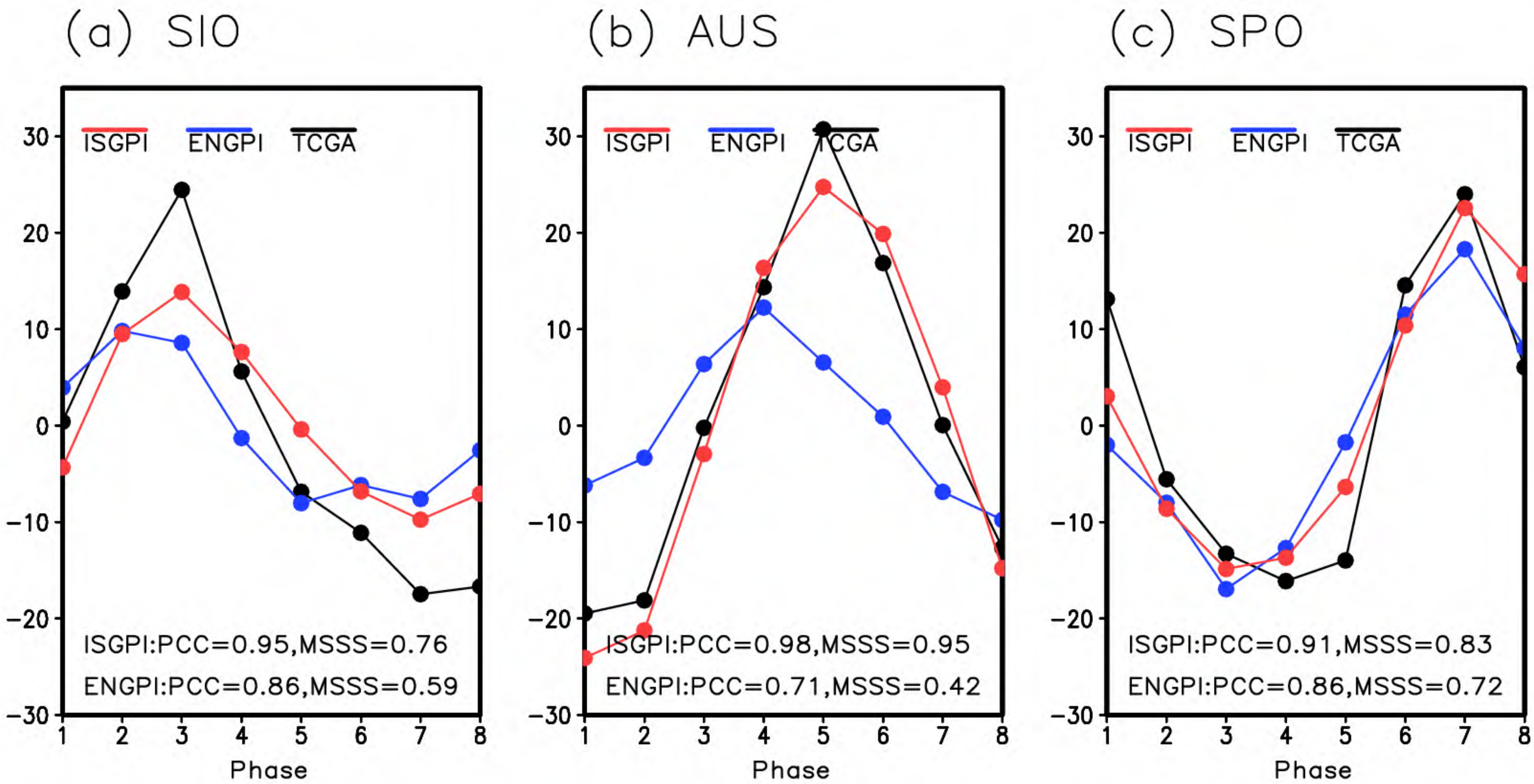

ISGPI, ENGPI, TCGA (OBS)

Performance in the tropics

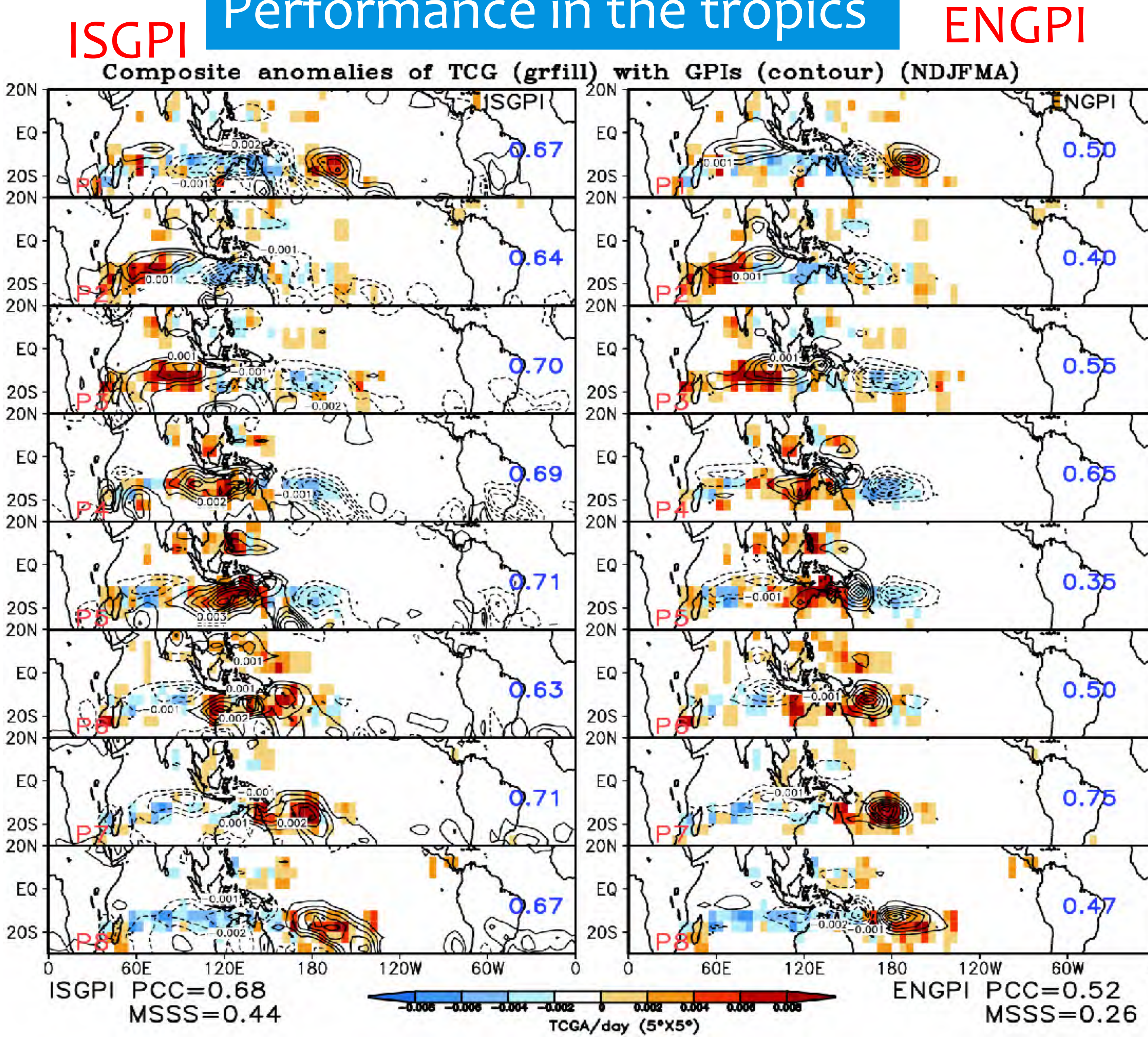

Remarkable MJO modulation of TCG probability at three TCG hot spots

70-80E **110-120E** **170-180E**

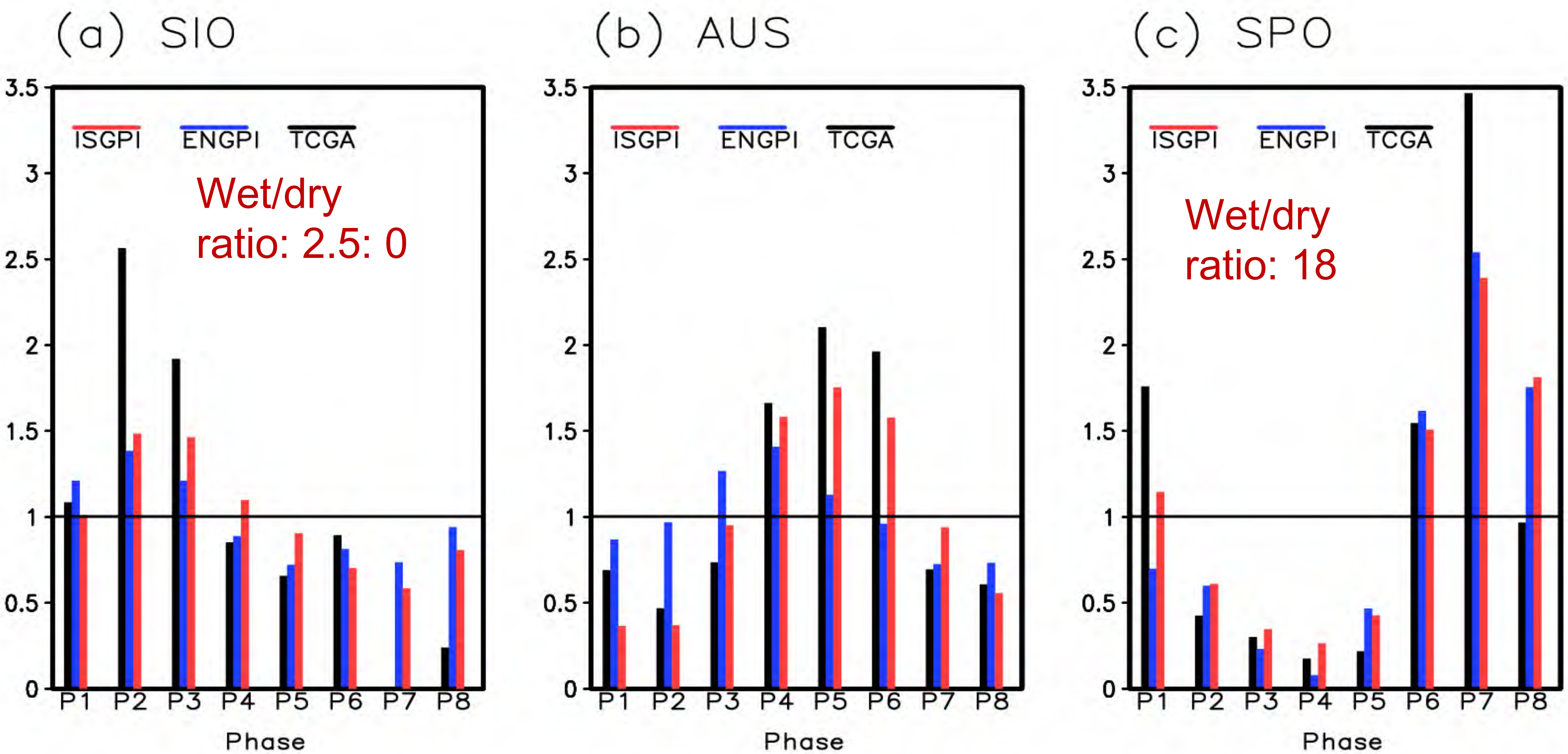

MJO modulation in SPO: Wet phase probability increased to 3.5 times, dry phases decreased to 0.2 times.

Conclusions

* During Austral summer, the most effective large scale MJO control of TCG is $f\zeta_{r850}$, and ω_{500} is also important.
* The new ISGPI represents ISVs of TCGF significantly better than the climatological GPI.
* MJO modulates TC genesis primarily through changing low-level vorticity induced by its Rossby wave gyres and the meridional shears of the equatorial zonal wind anomalies.
* In the hot spots of TC genesis, the probability of TC genesis are remarkably regulated by the wet and dry phases of MJO. Application of the new ISGPI might have a good potential to improve dynamical sub-seasonal prediction of TCG.

Implications

* The large scale factors controlling TCG on various time scales may differ, thus, the climatological GPI need to be modified when applying to diagnoses of climate variability and perhaps future change of TCG potential.
* The dynamical model-simulated MJO low-level circulation structure and its eastward propagation are both critically important in determining its impact on TC genesis.

BSISO modulation of TC genesis:
An intraseasonal genesis potential index

1-23 2017 AMS Seattle

BSISV modulation of TCG potential (MJJASO, 1979-2015)

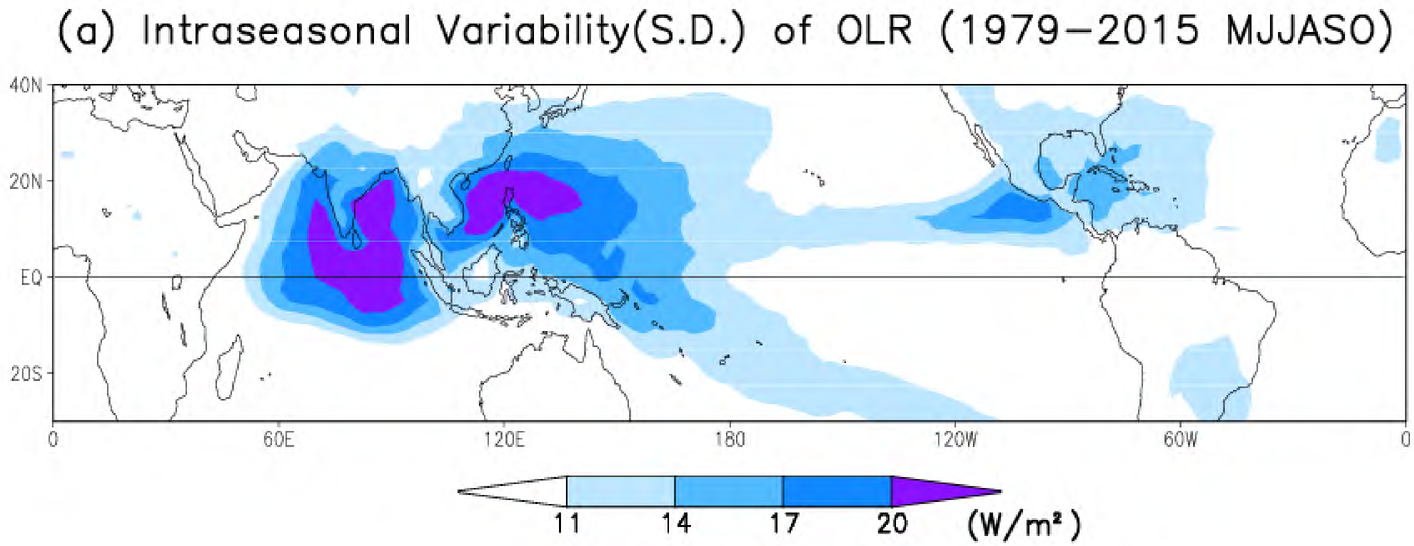

“ The major intraseasonal OLR variability is shifted to the Northern Hemisphere (NH) mostly between the equator and 25N “

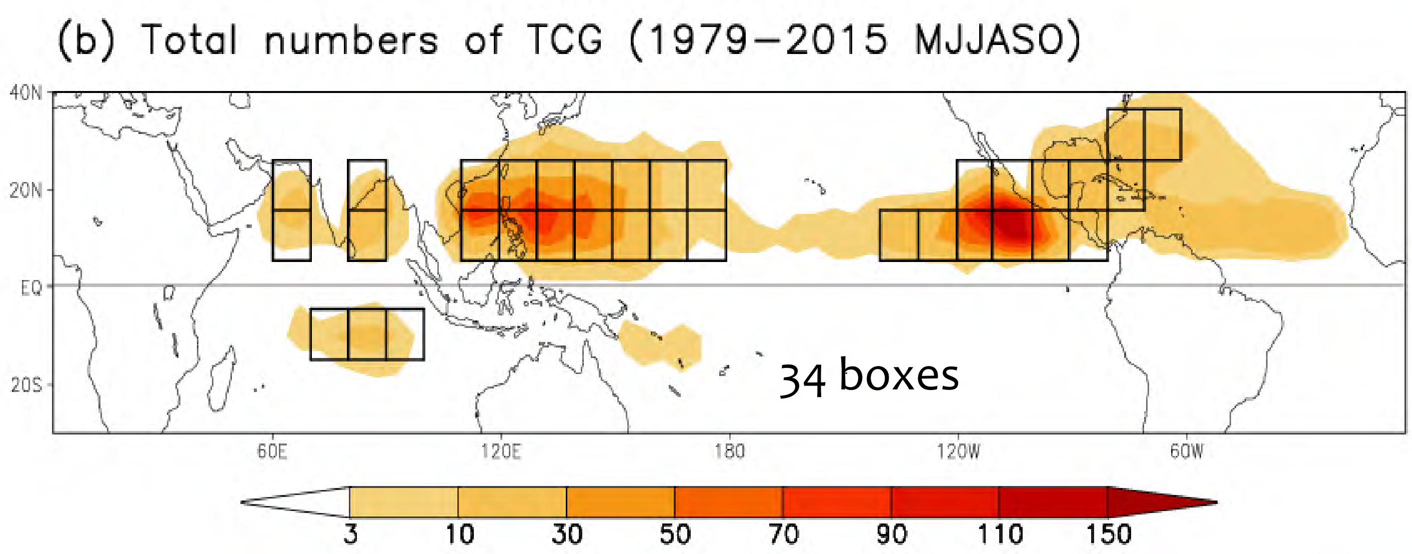

“The TCG also primarily occurs between 10N and 25N”

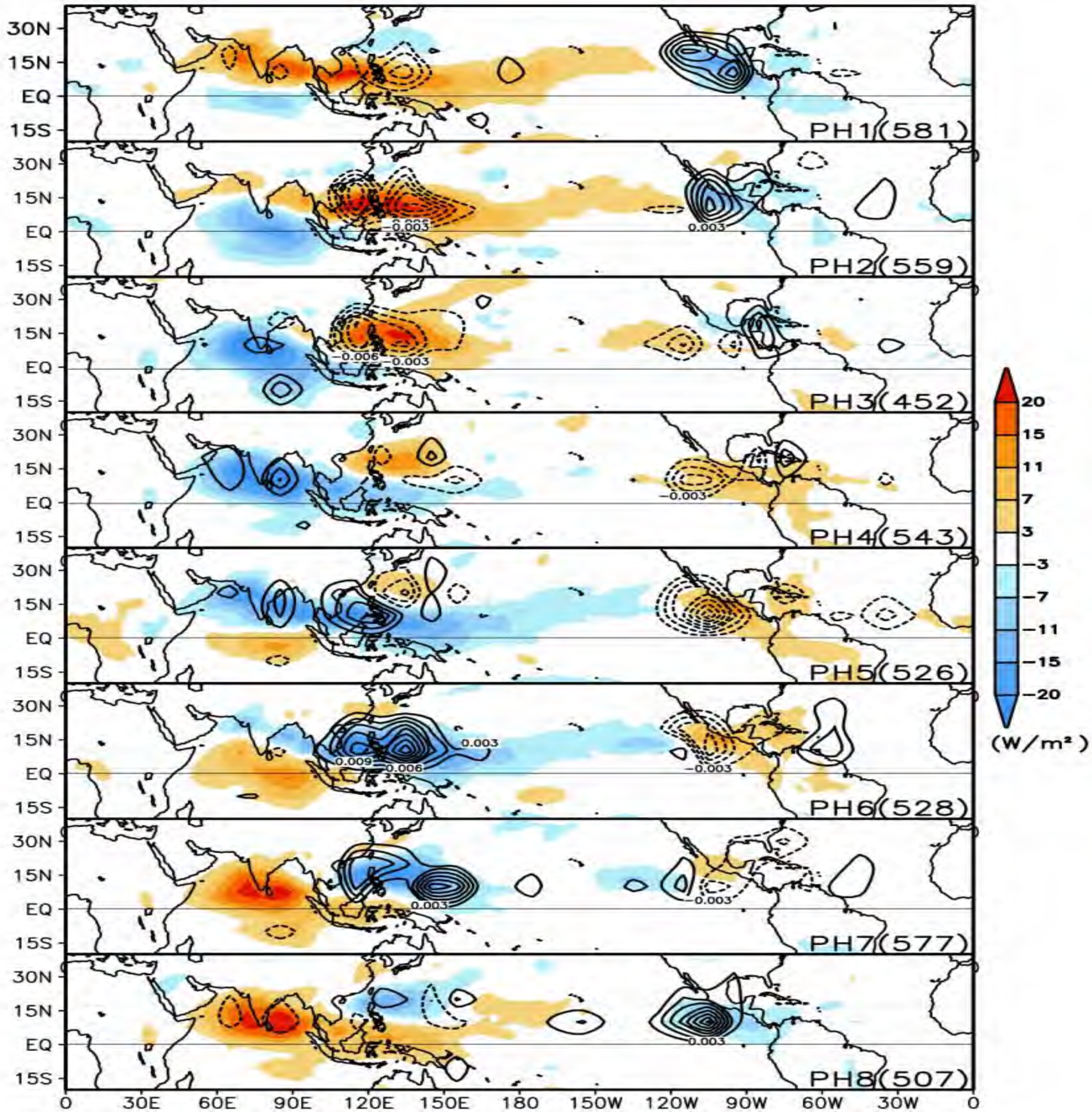

Eight-phase composite IS anomalies of OLR (shading) and TCGF (contour, TC number per day) during MJJAS) of 1979~2015.

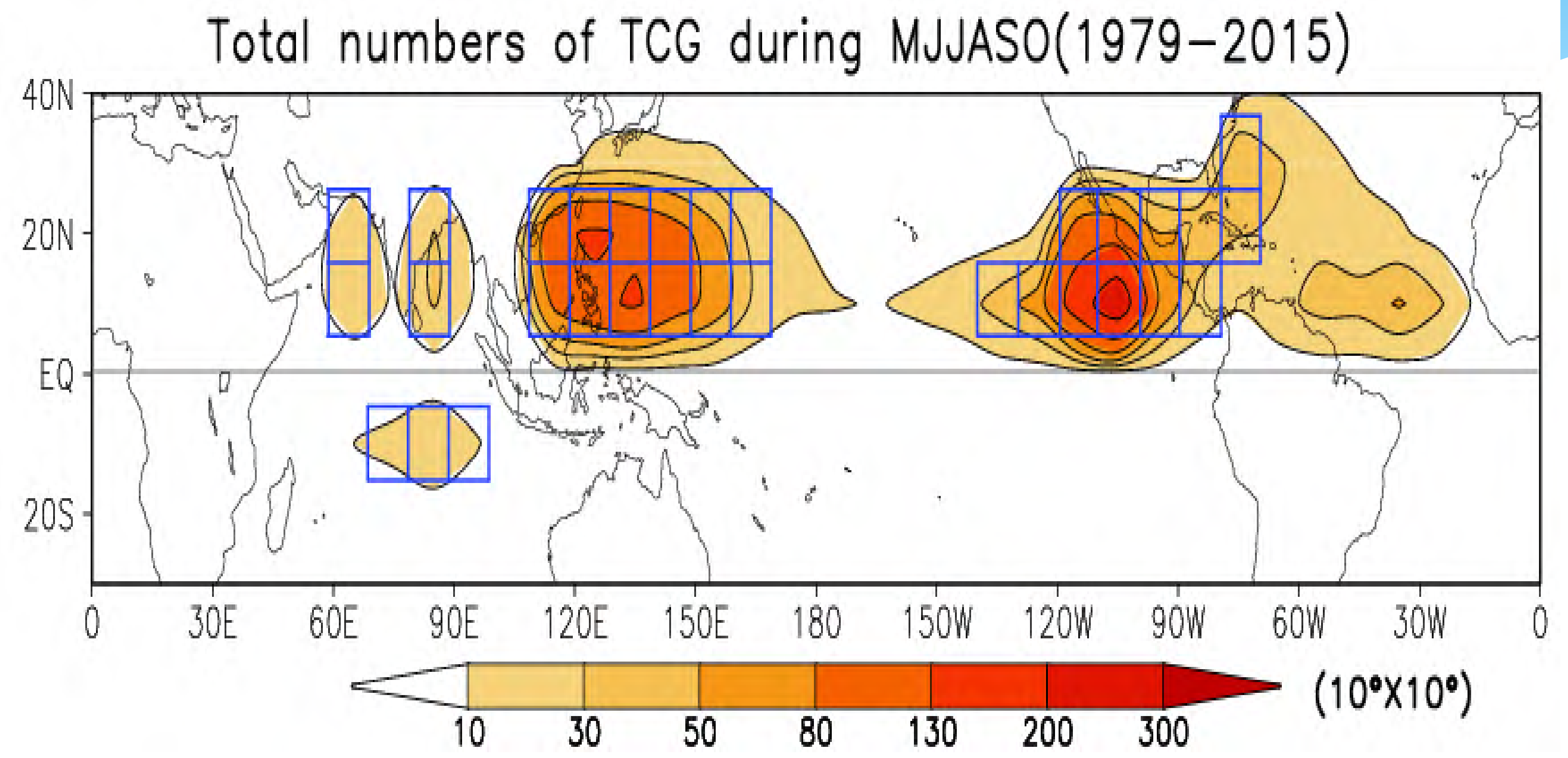
Total numbers of TCG during MJJASO(1979-2015)
40N
20N
EQ
20S
0
30E
60E
90E
120E
150E
180
150W
120W
90W
60W
30W
0
10
30
50
80
130
200
300
(10°X10°)

10 candidate factors

(EQ-20°N)	$TCGF$	V_{pot}	η_{850}	RH_{600}	V_s	SST_a	U_{x850}	U_{y500}	V_{zs}	$f\zeta_{r850}$	ω_{500}
$TCGF$	**1.00**	-0.15	**0.61**	**0.61**	-0.10	**-0.22**	**-0.45**	**-0.60**	**-0.38**	**0.60**	**-0.68**
V_{pot}	-0.15	**1.00**	**-0.22**	-0.01	-0.05	**0.72**	-0.17	**0.24**	**0.49**	**-0.34**	0.01
η_{850}	**0.61**	-0.22	**1.00**	**0.69**	-0.07	-0.13	**-0.39**	**-0.86**	**-0.22**	**0.97**	**-0.74**
RH_{600}	**0.61**	-0.01	**0.69**	**1.00**	-0.05	**-0.18**	**-0.68**	**-0.63**	**-0.26**	**0.61**	**-0.94**
V_s	-0.10	-0.05	-0.07	-0.05	**1.00**	0.03	0.06	0.03	0.03	-0.06	0.04
SST_a	**-0.22**	**0.72**	-0.13	**-0.18**	0.03	**1.00**	0.08	0.11	**0.56**	**-0.24**	0.16
U_{x850}	**-0.45**	-0.17	**-0.39**	**-0.68**	0.06	0.08	**1.00**	**0.31**	0.10	**-0.27**	**0.68**
U_{y500}	**-0.60**	**0.24**	**-0.86**	**-0.63**	0.03	0.11	**0.31**	**1.00**	**0.33**	**-0.84**	**0.69**
V_{zs}	**-0.38**	**0.49**	**-0.22**	**-0.26**	0.03	**0.56**	0.10	**0.33**	**1.00**	**-0.30**	**0.21**
$f\zeta_{r850}$	**0.60**	**-0.34**	**0.97**	**0.61**	-0.06	**-0.24**	**-0.27**	**-0.84**	**-0.30**	**1.00**	**-0.66**
ω_{500}	**-0.68**	0.01	**-0.74**	**-0.94**	0.04	0.16	**0.68**	**0.69**	**0.21**	**-0.66**	**1.00**

The bold numbers indicate statistically significant at 95% confidence level. Samp le size is 248.

Stepwise regression- An anomalous GPI for IS variations of TCG (MJJASO)

MJO	V_{pot}	SST	RH_{600}	U_{x850}	U_{y500}	V_{zs}	V_s	$f^*\xi_{r850}$	w_{500}
R	-0.13	-0.21	0.60	-0.44	-0.59	-0.37	-0.10	0.59	-0.67
R(RH, W500)=-0.94									
20°S-EQ	Without NAT					0.74 [2]		0.74 [3]	0.69 [1]

$$ISGPI = (-0.52)^*\ \omega_{500} + (-0.23)^*\ V_{zs} + (0.20)^*\ f\zeta_{r850}$$

The ω_{500} has the highest contribution and its weight is nearly twice larger than other two factors (V_{zs} and $f\zeta_{r850}$).

The vertical shear of zonal winds, V_{zs} is relatively independent of $f\zeta_{r850}$ and ω_{500}.

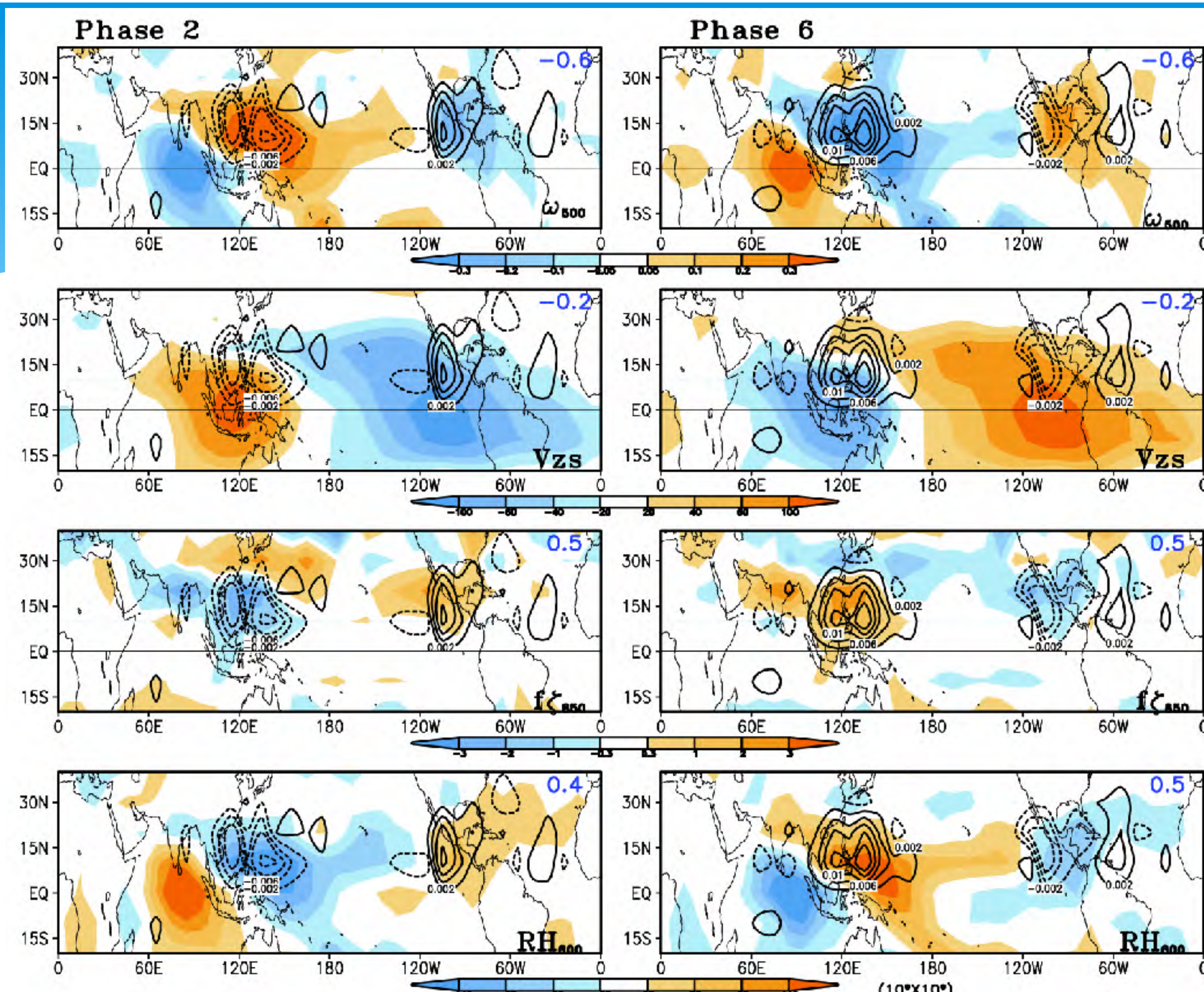

Fig. 3. Co… …ical wind shear(V_{zs}), relative vorticity at 850hPa multiplied by Coriolis force ($f\zeta_{r850}$), and relative humidity at 600hPa (RH_{600}) (in shading) at BSISO Phase 2 and 6 during northern hemisphere summer (MJJASO) of 1979~2015. The tropical cyclone genesis frequency (TCGF) anomaly (number/day) is plotted in black contour. $f\zeta_{r850}$ is scaled by 10^5. Pattern correlation coefficient between each variable and TCGF anomaly is shown at the upper-right corner.

Global and regional indices

Region	ω_{500}	V_{zs}	$f\zeta_{r850}$	Equation
Globe	0.68^{1}	0.72^{2}	0.74^{3}	$(-0.51)*\omega_{500} + (0.20)*f\zeta_{r850} + (-0.21)*V_{zs}$
IO	0.72^{1}	0.79^{3}	0.78^{2}	$(-0.56)*\omega_{500} + (0.32)*f\zeta_{r850} + (-0.12)*V_{zs}$
WNP	0.75^{1}	0.78^{2}	0.80^{3}	$(-0.55)*\omega_{500} + (0.22)*f\zeta_{r850} + (-0.20)*V_{zs}$
ENP	0.81^{1}	0.84^{3}	0.84^{2}	$(-0.67)*\omega_{500} + (0.24)*f\zeta_{r850} + (-0.02)*V_{zs}$
Western NAT	0.49^{3}	0.48^{2}	0.45^{1}	$(-0.16)*\omega_{500} + (0.46)*f\zeta_{r850} + (-0.25)*V_{zs}$

Table. 3. Results of stepwise selection of the influential factors for BSISO index and the multi-linear regression equation for globe and each basin. The numbers indicate complex correlation coefficients. The superscripts indicate the order of selection. The regression coefficients are normalized to reflect their relative contribution.

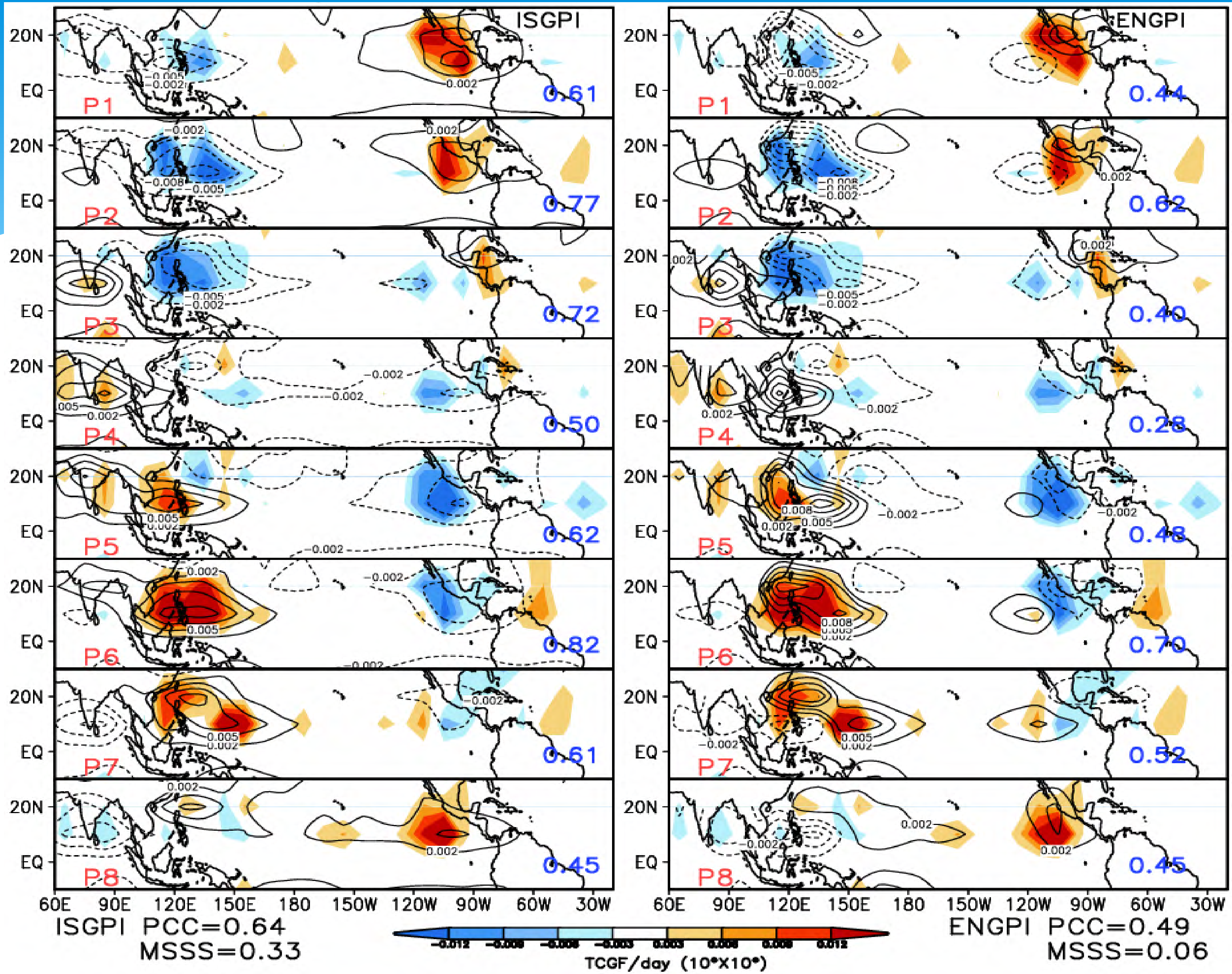
ISGPI
ENGPI
P1
P2
P3
P4
P5
P6
P7
P8
0.61
0.77
0.72
0.50
0.62
0.82
0.61
0.45
0.44
0.62
0.40
0.28
0.48
0.70
0.52
0.45
20N
EQ
60E 90E 120E 150E 180 150W 120W 90W 60W 30W
ISGPI PCC=0.64
MSSS=0.33
ENGPI PCC=0.49
MSSS=0.06
TCGF/day (10°X10°)

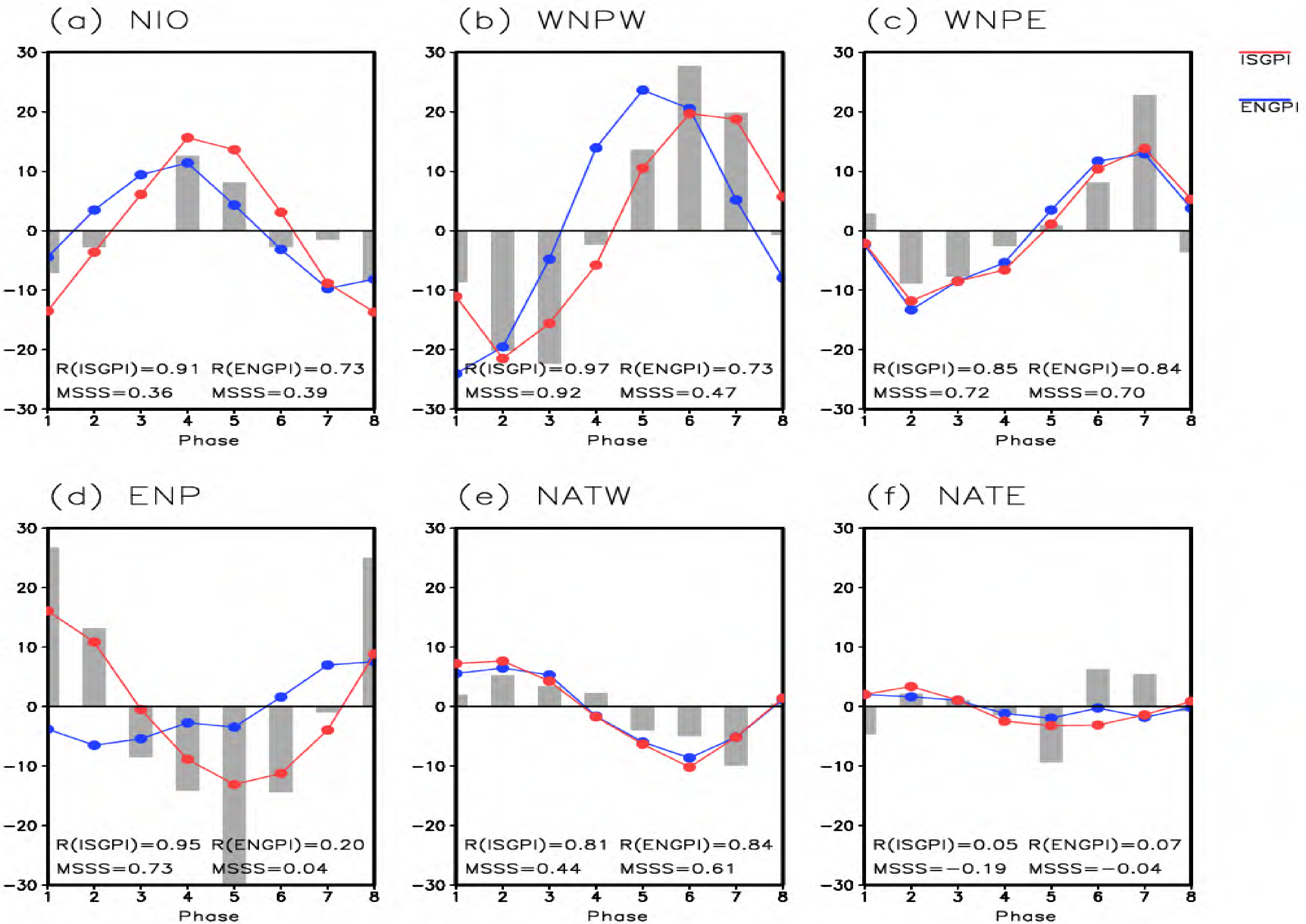
(a) NIO
R(ISGPI)=0.91 R(ENGPI)=0.73
MSSS=0.36 MSSS=0.39
(b) WNPW
R(ISGPI)=0.97 R(ENGPI)=0.73
MSSS=0.92 MSSS=0.47
(c) WNPE
R(ISGPI)=0.85 R(ENGPI)=0.84
MSSS=0.72 MSSS=0.70
ISGPI
ENGPI
(d) ENP
R(ISGPI)=0.95 R(ENGPI)=0.20
MSSS=0.73 MSSS=0.04
(e) NATW
R(ISGPI)=0.81 R(ENGPI)=0.84
MSSS=0.44 MSSS=0.61
(f) NATE
R(ISGPI)=0.05 R(ENGPI)=0.07
MSSS=−0.19 MSSS=−0.04
Phase

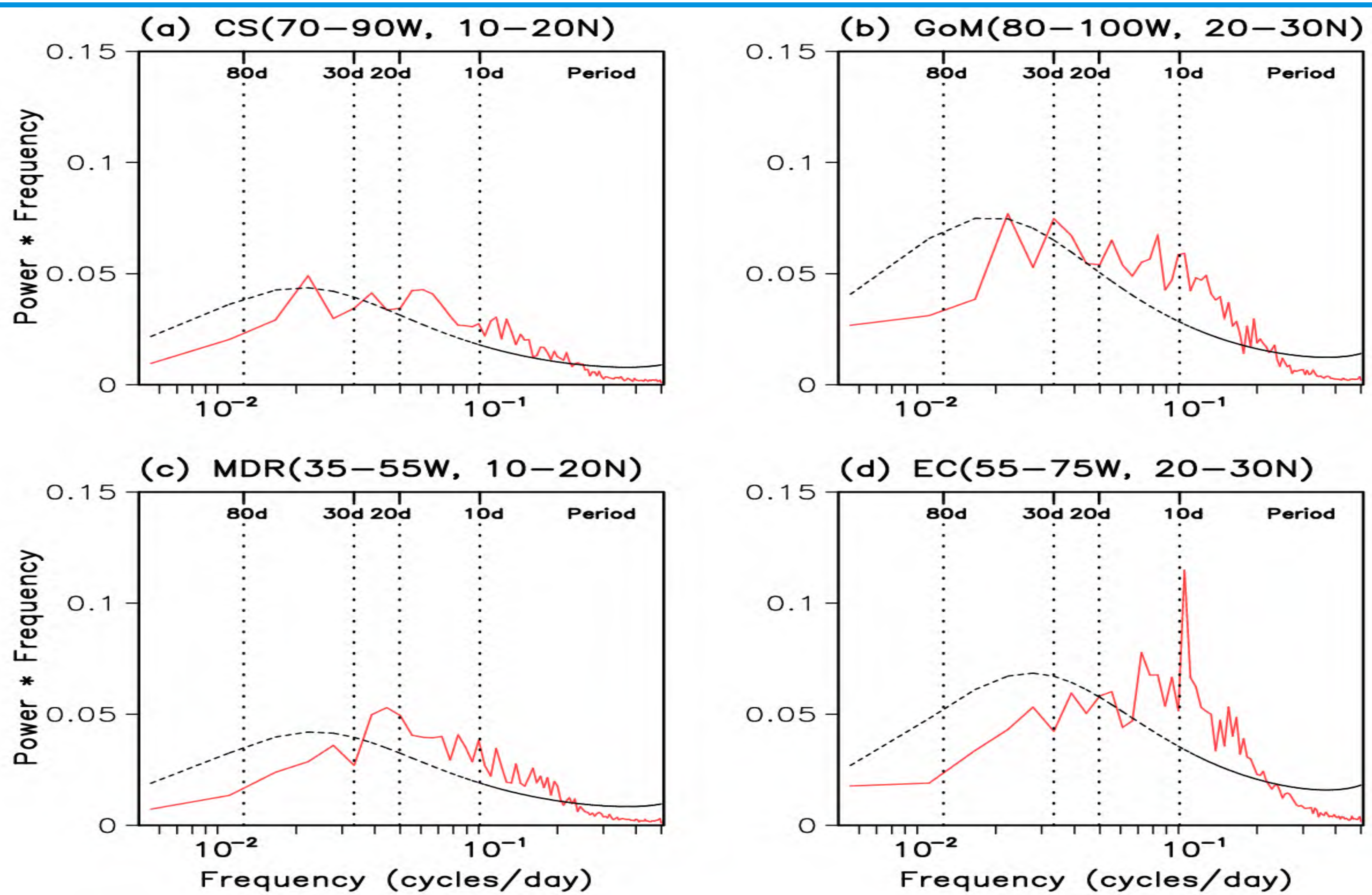

Fig. 6 Power spectra (solid line) of the upper-level (200hPa) zonal wind anomaly (daily climatology removed) over (a) Cari bbean Sea (70°-90°W, 10°-20°N), (b) Gulf of Mexico (80°-100°W, 20°-30°N), (c) Main Development Region (35°-55°W, 10°-20°N), and Eastern Coast of North America (55°-75°W, 20°-30°N) regions during NH summer (MJJASO) of 1979~20 15. The dashed curve is the red-noise spectrum in 90% confidence level.

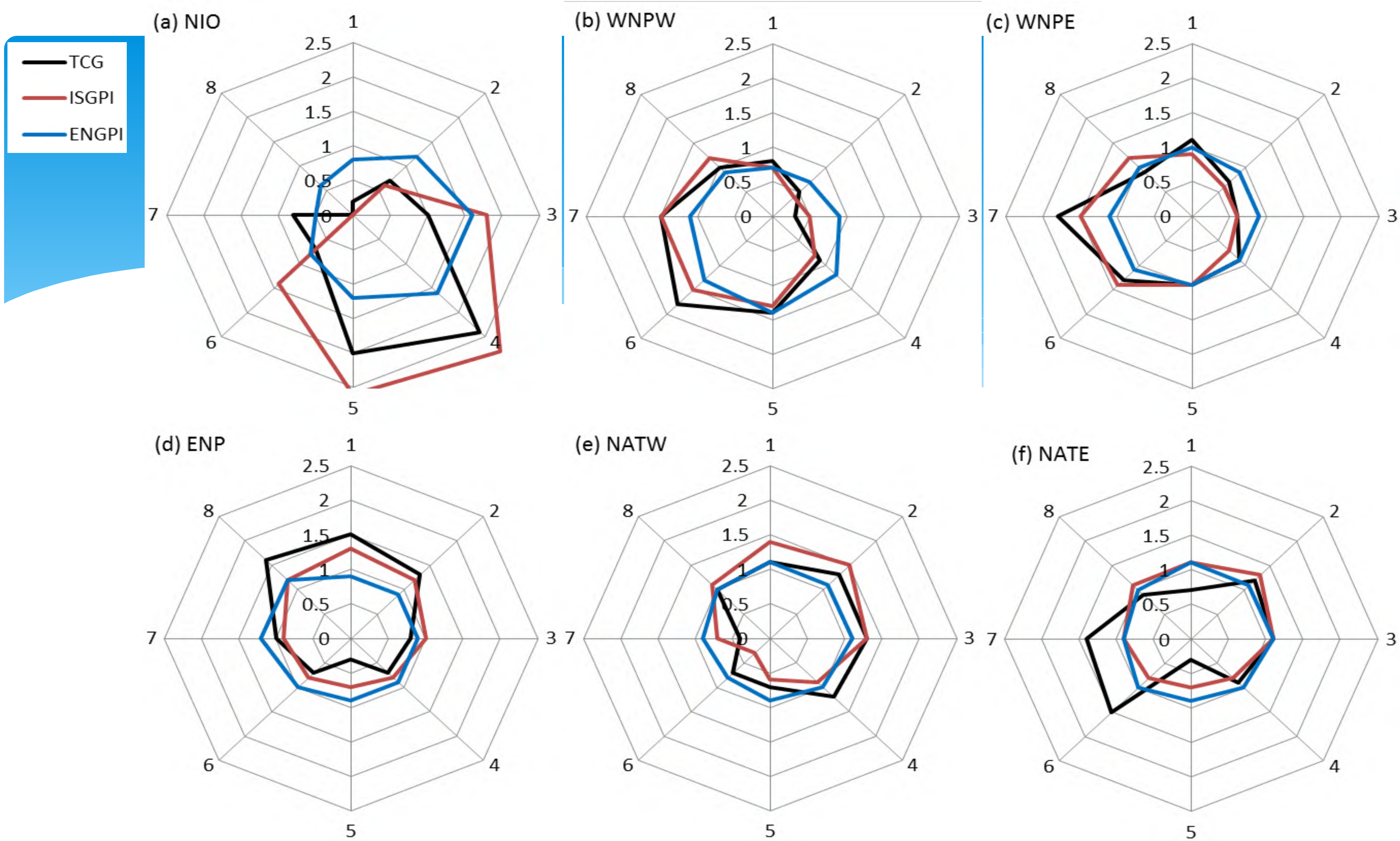

Fig. 7. The normalized TCG frequency (by its corresponding climatological mean TCG frequency at each sub-region) during composite eight phases (1 to 8) of BSISO in NH summer (MJJASO) of 1979~2015. results are derived from observation (black) and predicted by ISGPI (red) and ENGPI (blue) at six TCG zones in the Northern Ocean: (a) northern Indian Ocean (NIO, 60°-70°E, 80°-90°E, 5°-25°N), (b) western part of western North Pacific (WNPW, 110°-130°E, 5°-25°N), (c) eastern part of WNP (WNPE, 140°E-160°E, 5°-25°N), (d) eastern North Pacific (ENP, 100°-120°W, 5°-15°N, 110°-120°W, 15°-25°N), (e) western part of North Atlantic (NATW, 80°-90°W, 5°-15°N, 70°-100°W, 15°-25°N), and (f) eastern part of North Atlantic (NATE, 20°-60°W, 5°-15°N).

Table. 4. Results of stepwise selection of the influential factors for three BSISO indices: BSISO1 index (40°-160°E, 0°-40°N; OLR and U850), RMM(WH) index (0°E-360°, 15°S-15°N; OLR, U850, and U200), and OLR index (0°E-360°, 0°-20°N). The numbers indicate complex correlation coefficients. The superscripts indicate the order of selection.

BSISO Index	V_{pot}	SST_a	RH_{600}	U_{x850}	U_{y500}	V_{zs}	V_s	$f\zeta_{r850}$	ω_{500}
BSISO1					0.72^{2}	0.73^{3}			0.68^{1}
RMM(WH)						0.68^{2}		0.70^{3}	0.61^{1}
$OLR_{0°\text{-}20°N}$						0.72^{2}		0.74^{3}	0.68^{1}

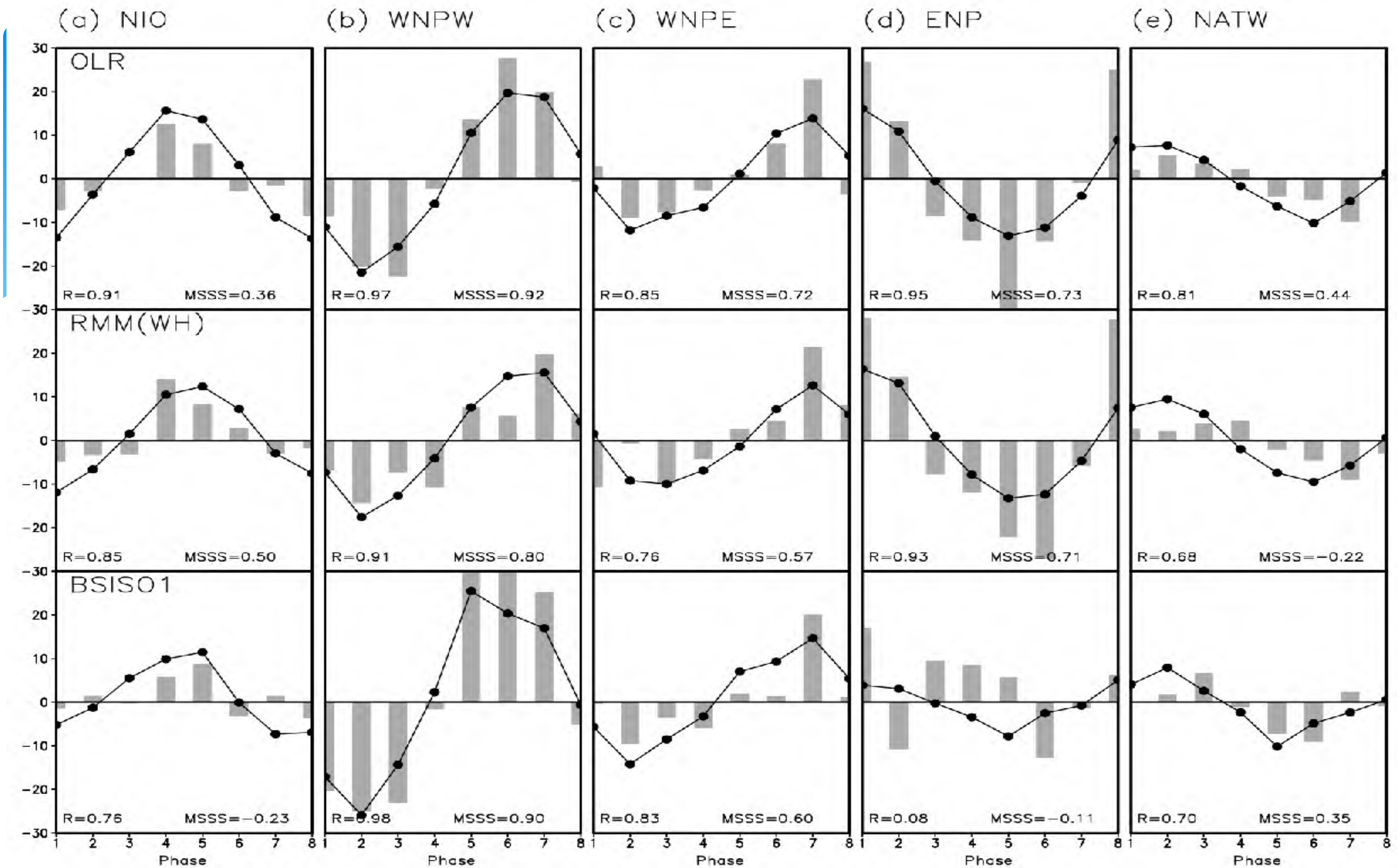

Fig. 8 Performance of the ISGPI (black curves) by three different BSISO indices (OLR, RMM, BSISO1) in reproducing observed TC genesis number (black bar) in five sub-regions of Northern Ocean: (a) northern Indian Ocean (NIO, 60°-70°E, 80°-90°E, 5°-25°N), (b) western part of western North Pacific (WNPW, 110°-130°E, 5°-25°N), (c) eastern part of WNP (WNPE, 140°E-160°E, 5°-25°N), (d) eastern North Pacific (ENP, 100°-120°W, 5°-15°N, 110°-120°W, 15°-25°N), and (e) western part of North Atlantic (NATW, 80°-90°W, 5°-15°N, 70°-100°W, 15°-25°N) during composite eight phases (P1 to P8) of BSISO in boreal summer (MJJASO) of 1979~2015.

Thank you!
Any comments?

Major processes by which MJO regulates TCG

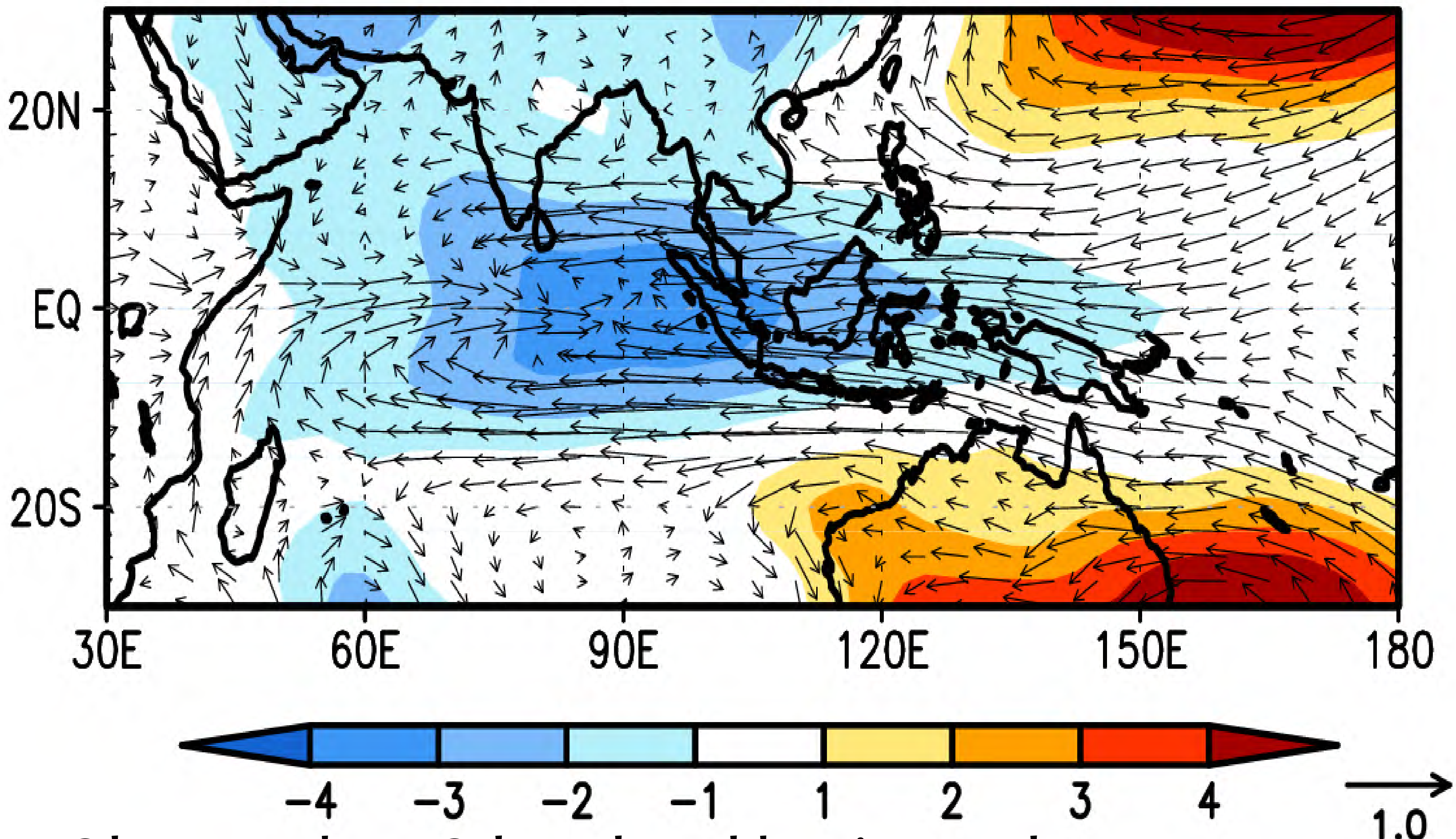

Observed MJO low-level horizontal structure

The observed 850-hPa wind (ms^{-1}, vector) and zonal wind speed (ms^{-1}, shading). with reference to the precipitation anomaly over (10S-10N, 80E-100E). The wind strengths are scaled to a fixed 3mm/day precipitation rate.

An IS AGPI

$$\text{IS AGPI} = (0.68)^* f\zeta_{r850} + (-0.37)^* \omega_{500} + (0.19)^* V_{zs}$$

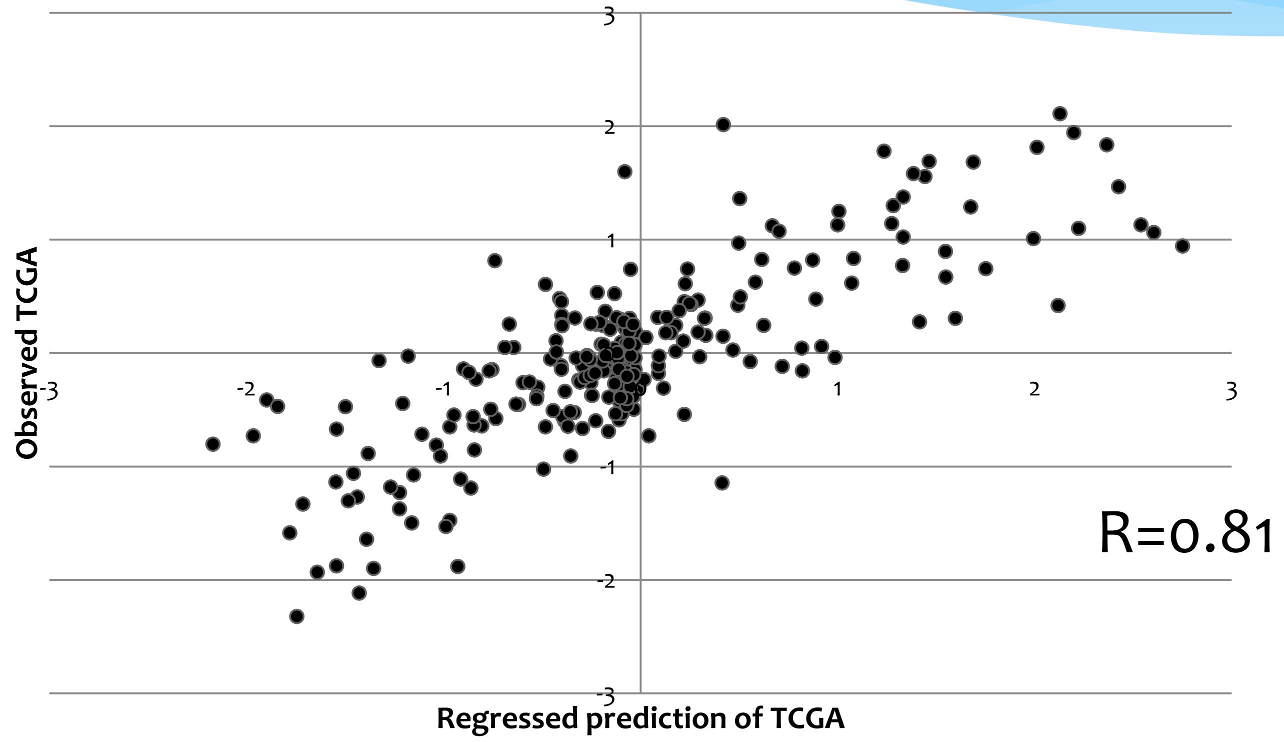

Correlation coefficient Tablle

(20S-EQ)	*TCGF*	V_{pot}	SST_a	RH_{600}	U_{x850}	U_{y500}	V_{zs}	V_s	$f\zeta_{r850}$	ω_{500}
TCGF	1.000	-0.275	-0.138	***0.553***	-0.254	***-0.539***	-0.418	-0.014	***0.726***	***-0.660***
V_{pot}	-0.275	1.000	0.473	0.035	-0.289	0.295	***0.713***	-0.014	***-0.533***	0.106
SST_a	-0.138	0.473	1.000	0.261	-0.422	0.423	0.351	-0.058	-0.388	-0.135
RH_{600}	***0.553***	0.035	0.261	1.000	***-0.747***	-0.177	-0.144	0.046	0.327	***-0.924***
U_{x850}	-0.254	-0.289	-0.422	***-0.747***	1.000	-0.080	-0.204	0.009	0.093	***0.659***
U_{y500}	***-0.539***	0.295	0.423	-0.177	-0.080	1.000	***0.510***	-0.061	***-0.802***	0.254
V_{zs}	0.418	***0.713***	0.351	-0.144	-0.204	***0.510***	1.000	-0.028	***-0.748***	0.260
V_s	-0.014	-0.014	-0.058	0.046	0.009	-0.061	-0.028	1.000	0.029	-0.005
$f\zeta_{r850}$	***0.726***	***-0.533***	-0.388	0.327	0.093	***-0.802***	***-0.748***	0.029	1.000	***-0.503***
ω_{500}	***-0.660***	0.106	-0.135	***-0.924***	***0.659***	0.254	0.260	-0.005	***-0.503***	1.000

- The vertical shear Vs and MPI V_{pot} are not important!
- RH600 is the best among ENGPI factors but highly related to W_{500} (r=-0.92)
- Vertical shear of zonal winds is better than the total wind shear

Results of stepwise selection of the influential factors for each BSISO (OLR) index The superscript numbers indicate the order of selection.

BSISO index (OLR)	V_{pot}	SST_a	RH_{600}	U_{x850}	U_{y500}	V_{zs}	V_s	$f\zeta_{r850}$	ω_{500}
30°S-30°N						0.653^{2}		0.666^{3}	0.596^{1}
20°S-20°N						0.658^{2}		0.671^{3}	0.591^{1}
15°S-15°N						0.655^{2}		0.663^{3}	0.597^{1}
EQ-15°N						0.704^{2}		0.718^{3}	0.658^{1}
EQ-20°N						**0.716^{2}**		**0.732^{3}**	**0.673^{1}**
EQ-30°N						0.707^{2}		0.723^{3}	0.667^{1}

$$ISGPI = (-0.495)^{*}\ \omega_{500} + (-0.216)^{*}\ V_{zs} + (0.208)^{*}\ f\zeta_{r850}$$

The ω_{500} has the highest contribution and its weight is nearly twice larger than other two factors (V_{zs} and $f\zeta_{r850}$).

The vertical shear of zonal winds, V_{zs} is relatively independent of $f\zeta_{r850}$ and ω_{500}. (Table 1)

Numbers of TCG along 10S-20S by MJO phase 1 to 8

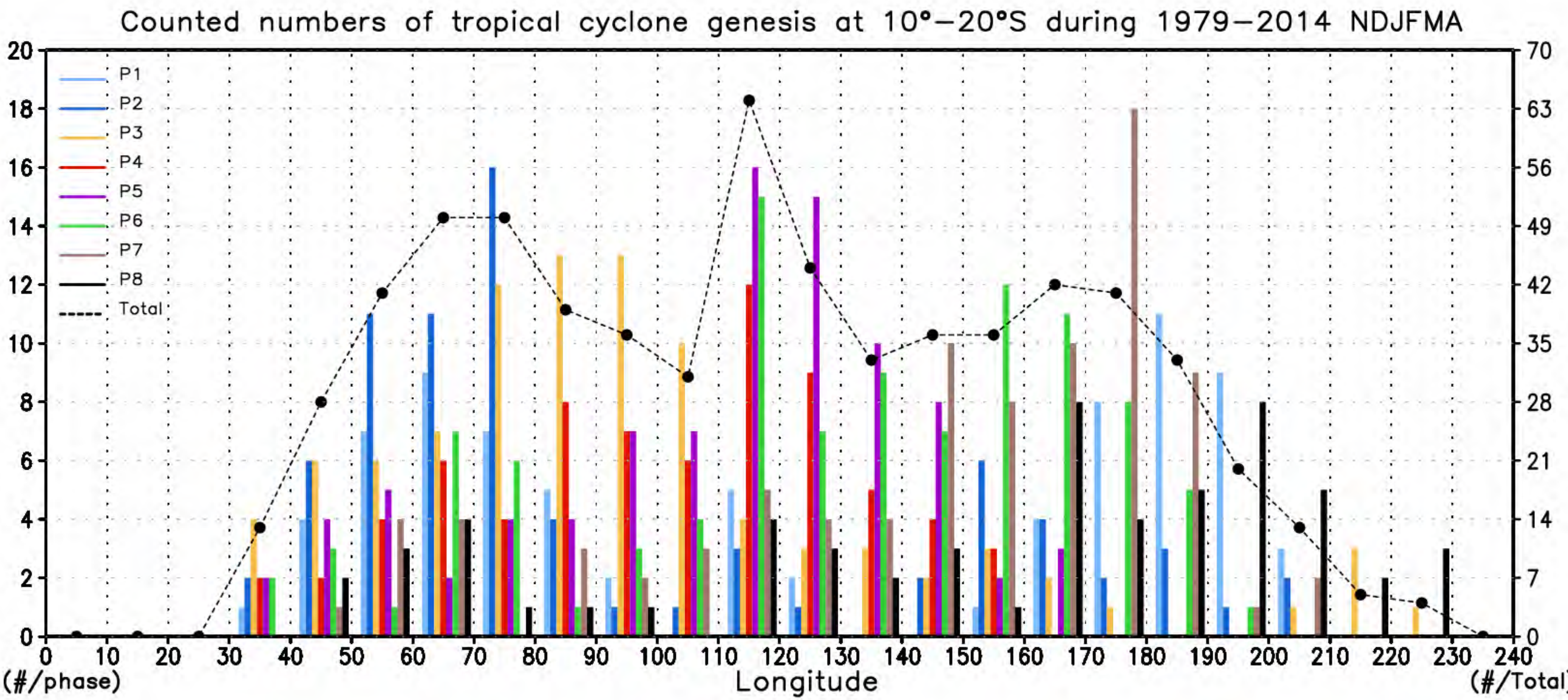

Sensitivity to choice of MJO indices

MJO index	V_{pot}	SST_a	RH_{600}	U_{x850}	U_{y500}	V_{zs}	V_s	$f\zeta_{r850}$	ω_{500}
OLR (0°-20°S)						0.811 ^{3}		0.726 ^{1}	0.802^{2}
$\boldsymbol{\Delta\chi_{850\text{-}150}}$ (90°S-90°N)				0.679 ^{3}				0.671 ^{2}	0.633^{1}
RMM (OLR,U850,U200) (15°S-15°N mean)								0.706 ^{2}	0.607^{1}

Sensitivity to OLR index definition

MJO	V_{pot}	SST	RH_{600}	U_{x850}	U_{y500}	V_{zs}	V_s	$f\zeta_{r850}$	w_{500}
30°S-30°N						0.752^{3}		0.743^{2}	0.643^{1}
20°S-20°N						0.757^{3}		0.645^{1}	0.748^{2}
15°S-15°N						0747^{3}		0.653^{1}	0.739^{2}
15°S-EQ						0.786^{3}		0.701^{1}	0.778^{2}
20°S-EQ						$\mathbf{0.811}^{3}$		$\mathbf{0.726}^{1}$	$\mathbf{0.802}^{2}$
30°S-EQ						0.803^{3}		0.701^{1}	0.792^{2}

Stepwise selection of the influential factors for each MJO index obtained from horizontal latitudinal range of 30°S-30°N, 20°S-20°N, 15°S-15°N, 15°S-EQ, 20°S-EQ, and 30°S-EQ. The real numbers indicate complex correlation coefficients.
The superscript numbers indicate the order of selection.

To focus on NAT region, EEOF over western hemisphere (25-60day) is analyzed. Using the eeof coefficients, 8-phase composite is obtained.

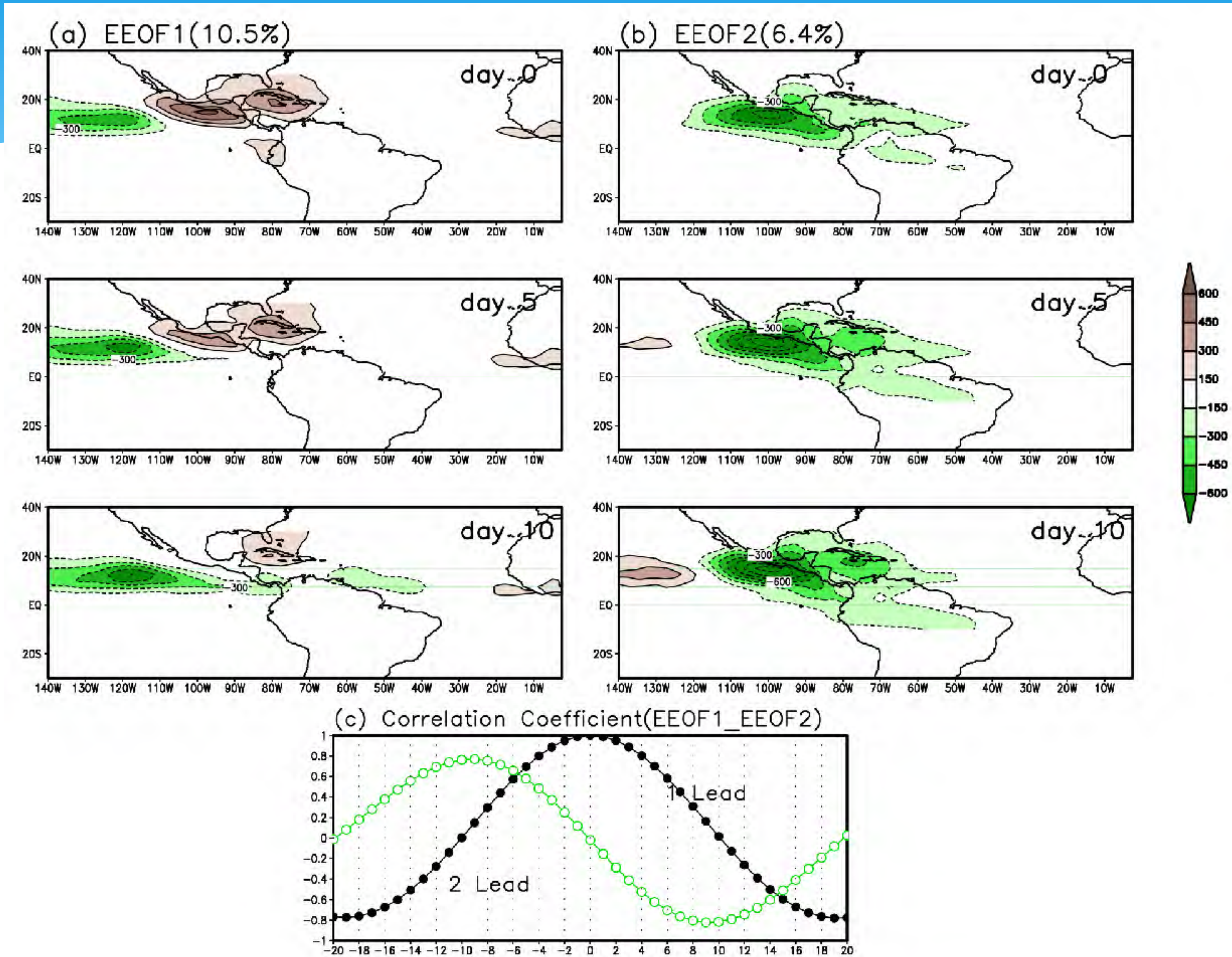

8-phase composite map using EEOF time coefficient.
The convection over the NAT region is more strongly displayed.

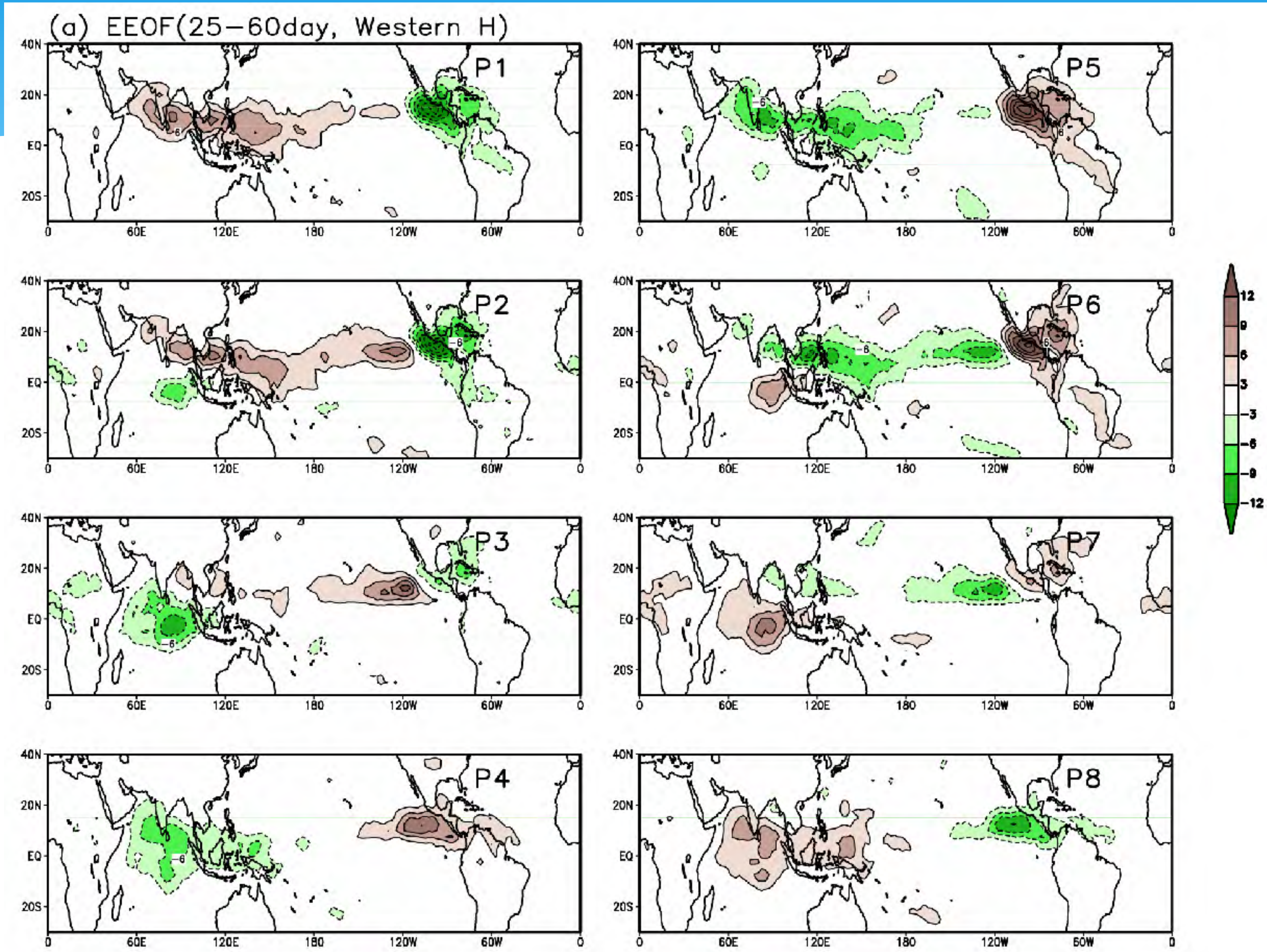

Normalized scattering diagrams

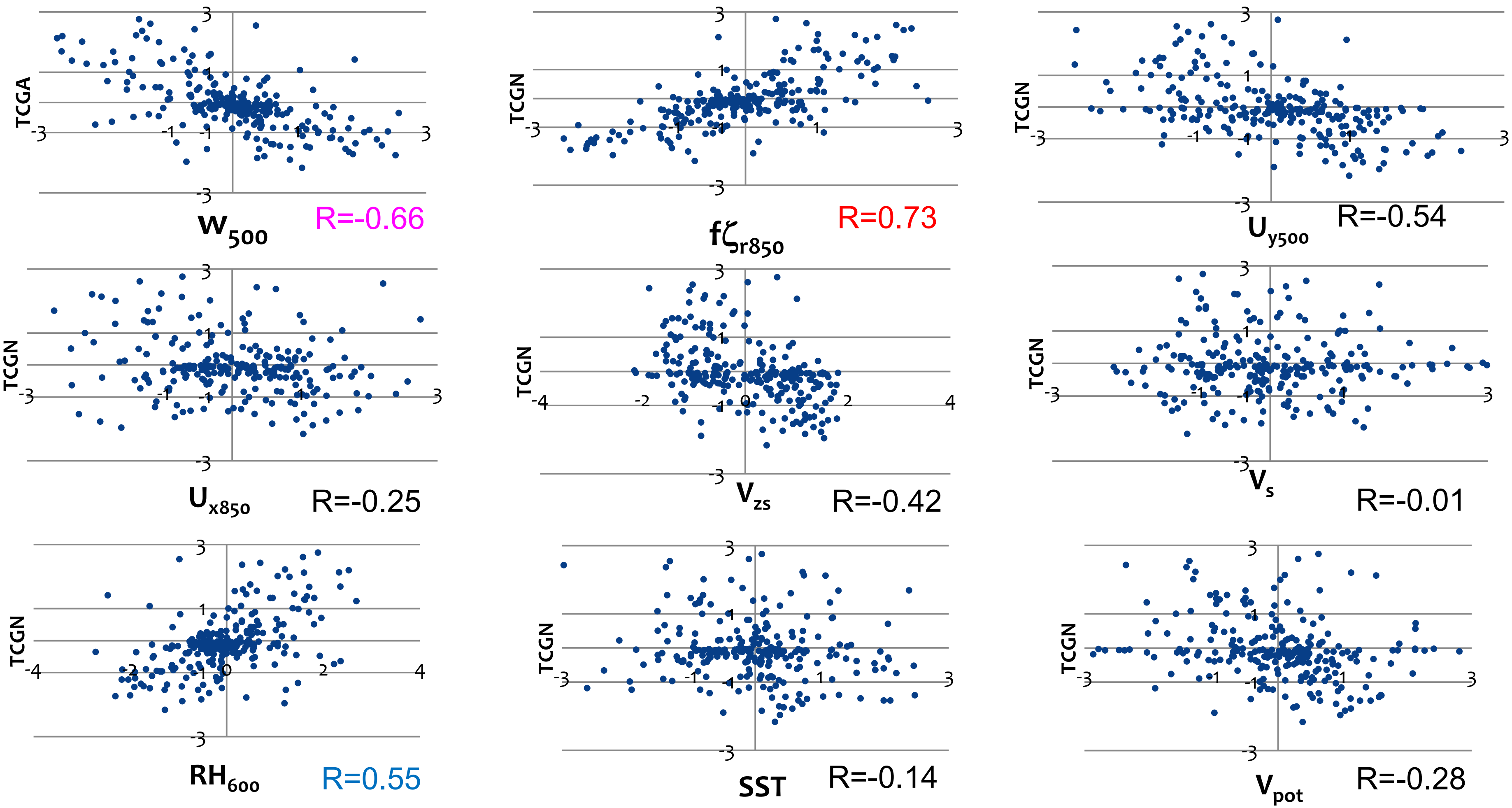

The normalized scattered diagram between anomalous tropical cyclone genesis (TCGA) and large scale factors (w_{500}, $f\zeta_{r850}$, U_{y500}, U_{x850}, V_{zs}, V_s, RH_{600}, SST, and V_{pot}) derived from 248 (8phase x 31 grid cells in Fig. 2b) of 10-degree grid cells.